Reassessment of body temperature and thermoregulation strategies in Mesozoic marine reptiles

Nicolas Séon, Peggy Vincent, Lene Liebe Delsett, Eve Poulallion, Guillaume Suan, Christophe Lécuyer, Aubrey Jane Roberts, François Fourel, Sylvain Charbonnier, Romain Amiot

Paleobiology

www.cambridge.org/pab

Reassessment of body temperature and thermoregulation strategies in Mesozoic marine reptiles

Nicolas Séon[1,2], Peggy Vincent[1], Lene Liebe Delsett[3], Eve Poulallion[2], Guillaume Suan[2], Christophe Lécuyer[2], Aubrey Jane Roberts[3], François Fourel[4], Sylvain Charbonnier[1] and Romain Amiot[2]

[1]Centre de Recherche en Paléontologie–Paris (CR2P), CNRS, Muséum national d'Histoire naturelle, Sorbonne Université, 57 rue Cuvier, 75231 Paris CEDEX 05, France
[2]Université Claude Bernard Lyon1, LGL-TPE, UMR 5276, CNRS, ENSL, UJM, F-69622, Villeurbanne, France
[3]Natural History Museum, University of Oslo, Norway
[4]Laboratoire d'Ecologie des Hydrosystèmes Naturels et Anthropisés, CNRS UMR 5023, Université Claude Bernard Lyon 1, Villeurbanne, France

Article

Cite this article: Séon, N., P. Vincent, L. L. Delsett, E. Poulallion, G. Suan, C. Lécuyer, A. J. Roberts, F. Fourel, S. Charbonnier, and R. Amiot (2025). Reassessment of body temperature and thermoregulation strategies in Mesozoic marine reptiles. *Paleobiology*, 1–21. https://doi.org/10.1017/pab.2025.2

Received: 18 July 2024
Revised: 24 December 2024
Accepted: 02 January 2025

Corresponding author:
Nicolas Séon;
Email: nicolasseon517@gmail.com

Handling Editor:
Erin Saupe

Abstract

Ichthyosauria, Plesiosauria, and Metriorhynchidae were apex predators in Mesozoic oceanic trophic networks. Previous stable oxygen isotope studies suggested that several taxa belonging to these groups were endothermic and that some of them were homeothermic organisms. However, these conclusions remain contentious owing to the associated uncertainties regarding the $\delta^{18}O$ value and oxygen isotope fractionation relative to environmental seawater. Here, we present new bioapatite phosphate $\delta^{18}O$ values ($\delta^{18}O_p$) of Ichthyosauria, Plesiosauria, and Metriorhynchidae (Middle Jurassic to Early Cretaceous) recovered from mid- to high paleolatitudes to better constrain their thermophysiology and investigate the presence of regional heterothermies. The intraskeletal $\delta^{18}O_p$ variability failed to reveal distinct heterothermic patterns within any of the specimens, indicating either intrabody temperature homogeneity or an overriding diagenetic overprint of the original biological $\delta^{18}O_p$ bone record. Body temperature estimates have been reassessed from new and published $\delta^{18}O_p$ values of well-preserved isolated teeth, recently revised Mesozoic latitudinal $\delta^{18}O$ oceanic gradients, and ^{18}O-enrichment factors of fully aquatic air-breathing vertebrates. Our results confirm that Ichthyosauria were homeothermic endotherms (31°C to 41°C), while Plesiosauria were likely poikilothermic endotherms (27°C to 34°C). The new body temperature estimates of the Metriorhynchidae (25°C to 32°C) closely follow ambient temperatures and point to poikilothermic strategy with no or little endothermic ability. These results improve our understanding of Mesozoic marine reptile thermoregulation and indicate that due to their limited body temperature variations, the $\delta^{18}O_p$ values from Ichthyosauria fossil remains could be used as valuable archives of Mesozoic oceans $\delta^{18}O_{sw}$ values that may help improve paleoenvironmental and paleoclimatic reconstructions.

Non-technical Summary

Some marine reptiles from the Mesozoic, such as ichthyosaurs, plesiosaurs, and metriorhynchids, were capable of reaching elevated body temperatures, and some could maintain body temperatures a few degrees above those of their marine environments, a characteristic similar to that observed in modern cetaceans. Nevertheless, the estimation of their body temperatures from the chemical oxygen signatures of their fossil remains (bones and teeth) is accompanied by uncertainties associated with the chemical oxygen signatures of the surrounding water and the mineralization processes of the bones and teeth. In this study, new data were collected from four ichthyosaurs, three plesiosaurs, and one metriorhynchid in order to gain a deeper understanding of the mechanisms by which these marine reptiles were able to maintain body temperatures higher than those of their environments. The chemical signatures of oxygen in the bones and teeth of the specimens did not exhibit any discernible patterns indicative of specific zones of heat production or loss, unlike what has been observed in modern marine vertebrates. Concurrently, we reassessed the estimated body temperatures of these marine reptiles, thereby corroborating the hypothesis that ichthyosaurs were homeothermic endotherms. Conversely, our new estimates suggest that plesiosaurs were likely poikilothermic endotherms, whereas metriorhynchids were probably also poikilothermic endotherms but with a limited capacity for heat production. Finally, the narrow range of body temperatures maintained by ichthyosaurs indicates that the oxygen chemical signatures of fossilized remains could serve as valuable markers for reconstructing variations in the oxygen isotope composition of the Mesozoic oceans, paving the way to enhance our understanding of the environment and climate of this period in Earth's history.

PALEOBIOLOGY
A PUBLICATION OF THE Paleontological SOCIETY

CAMBRIDGE UNIVERSITY PRESS

Introduction

During the Mesozoic Era (251.9 to 66.0 Ma), marine reptiles such as ichthyosaurs, plesiosaurs, and metriorhynchids were distributed worldwide and played a key role in the trophic networks. Paleobiogeographic (Kear 2006b; Bardet et al. 2014; Vavrek et al. 2014; Delsett et al. 2016; Rogov et al. 2019; Zverkov et al. 2021), osteohistological (Ichthyosauria: de Buffrénil and Mazin 1989, 1990; Anderson et al. 2019; Plesiosauria: Wiffen et al. 1995; Delsett and Hurum 2012; Fleischle et al. 2018), geochemical (Bernard et al. 2010; Séon et al. 2020; Leuzinger et al. 2023), and modeling studies (Brice and Grigg 2023) all indicate that Ichthyosauria Blainville, 1835 and Plesiosauria Blainville, 1835 were endothermic and probably homeothermic organisms, much like extant Cetacea Brisson, 1762. They would have been able to produce enough body heat to raise their body temperatures above those of the environments in which they lived (Bernard et al. 2010; Séon et al. 2020; Leuzinger et al. 2023). High and constant body temperature in Ichthyosauria would have been facilitated by their fusiform morphology favoring heat retention and the presence of a layer of fibroadipose tissue surrounding the trunk (Lindgren et al. 2018; Delsett et al. 2022). Evidence for adipose tissue is lacking for Plesiosauria, for which very few specimens preserving soft tissues have been found (Vincent et al. 2017). Thermophysiological studies of Metriorhynchidae Fitzinger, 1843, a group of fully aquatic marine Mesozoic crocodylomorphs, have not led to a consensus. The fossil occurrences confined to tropical paleolatitudes (Bardet et al. 2014) and the osteo-histological findings from studies by Hua and de Buffrénil (1996) and de Buffrénil et al. (2021) suggested that Metriorhynchidae had an ectothermic poikilothermic thermoregulatory strategy similar to that of modern crocodylomorphs. Conversely, the oxygen isotope analyses of Séon et al. (2020) suggested that Metriorhynchidae were able to raise their body temperatures a few degrees above that of the ambient environment by metabolic heat production but could not maintain a constant body temperature, indicating they were poikilothermic endotherms like extant tunas (Block and Finnerty 1994; Graham and Dickson 2004).

Previous estimates of body temperature reconstruction of Ichthyosauria, Plesiosauria, and Metriorhynchidae, calculated from the phosphate oxygen isotope composition of the bioapatite of their bones and teeth ($\delta^{18}O_p$), assumed a constant global oceanic $\delta^{18}O$ value ($\delta^{18}O_{sw}$) of $-1 \pm 1‰$ (Bernard et al. 2010; Séon et al. 2020; Leuzinger et al. 2023; Supplementary Information 1 for details about isotope-based body temperature estimations), an oversimplified assumption given latitudinal gradients in $\delta^{18}O_{sw}$ values recorded in Jurassic and Cretaceous seas (Alberti et al. 2017, 2020; Letulle et al. 2022). Furthermore, recent work has shown that the oxygen isotope compositions of body water from extant air-breathing fully marine species—*Orcinus orca* Linnæus, 1758, *Tursiops truncatus* Montagu, 1821 (Séon et al. 2023), and *Caretta caretta* Linnæus, 1758 (Séon 2023)—are less ^{18}O-enriched relative to their drinking water than that of semiaquatic vertebrates (crocodiles, turtles) used previously to reconstruct body temperatures of extinct marine reptiles (Bernard et al. 2010; Séon et al. 2020; Leuzinger et al. 2023).

Previous osteo-histological and geochemical studies were exclusively based on isolated teeth or bone remains (de Buffrénil and Mazin 1990; Bernard et al. 2010; Fleischle et al. 2018; Séon et al. 2020) and thus provided only partial information on the thermoregulation of Ichthyosauria, Plesiosauria, and Metriorhynchidae. A key aspect of thermophysiology is to define how constant body temperature is at the level of vital organs (homeotherm vs. poikilotherm; Clarke and Pörtner 2010; Furukawa et al. 2015; Lovegrove 2017) and the distribution of body temperature within the body, known as regional heterothermies (Irving and Hart 1957; Folkow and Blix 1987; Favilla et al. 2022). An investigation into the mechanisms employed by Ichthyosauria, Plesiosauria, and Metriorhynchidae to regulate their body temperatures allows for an understanding of their adaptation to their environments and the explanation of their stratigraphic occurrences in the fossil record in view of fluctuating environmental temperatures during the Mesozoic (Takashima et al. 2006; Dera et al. 2011; Wierzbowski et al. 2013). Such climate changes do not seem to have affected their diversity (Bardet 1994; Martin et al. 2014; Stubbs and Benton 2016). Moreover, precisely defining their thermoregulatory strategies opens the way to investigating their behavior. For instance, homeothermic endotherms are typically active organisms, as they are fully independent of the temperatures of their environments. Nevertheless, this requires a significant energy input (Clarke and Pörtner 2010). Conversely, some species that are considered to be regional endotherms can produce heat locally, which can result in temperature heterogeneities or regional heterothermies (Carey 1982; Block 1986; Dickson and Graham 2004; Graham and Dickson 2004). In swordfish, for example, the heat production located close to the eyes improves visual acuity in foraging cold environments of great depth (Block 1987; Fritsches et al. 2005), whereas heat production in locomotory muscles of tunas and lamnid sharks enables them to swim faster or migrate over longer distances than poikilothermic ectothermic organisms (Blank et al. 2007; Bernal et al. 2012; Watanabe et al. 2015; Harding et al. 2021). The mapping of intraindividual temperature variations, and thus regional heterothermies, through the use of oxygen isotopes enables the identification of heat-producing zones within an organism, in addition to the delineation of thermal windows, the preferred sites for heat loss, which serve to regulate body temperature (Séon et al. 2022, 2024).

In this study, we performed an oxygen isotope analysis of 239 bones and 8 teeth from complete or subcomplete specimens, enabling the first evaluation of possible regional heterothermies within the bodies of ichthyosaurs, plesiosaurs, and metriorhynchids. We also reassessed body temperature estimates of Ichthyosauria, Plesiosauria, and Metriorhynchidae using new and published $\delta^{18}O_p$ tooth data and an ^{18}O-enrichment of fully aquatic animals and considering a global $\delta^{18}O_{sw}$ gradient for the Jurassic and Cretaceous seas.

Institutional Abbreviations. MHNLM, Muséum d'Histoire Naturelle Le Mans; MPV, Musée Paléontologique de Villers-sur-Mer; PMO, Palaeontological collections of the Natural History Museum, University of Oslo, Norway.

Material and Methods

Sampled Specimens

Specimens of four Ichthyosauria, three Plesiosauria, and one Metriorhynchidae were sampled for their intraskeletal $\delta^{18}O_p$ variability; taxonomic affiliation, collection number, size estimate, stratigraphic age, locality, and type of sampled material for each marine reptile specimen are reported in Table 1. In addition to these complete and subcomplete specimens, two teeth of Metriorhynchidae indet. specimens from the Marnes de Dives Formation (late Callovian, Les Vaches Noires Cliffs, France) were sampled for their $\delta^{18}O_p$ values to reassess metriorhynchid body temperatures (Table 1), as well as a pachycormid fish tooth belonging to *Hypsocormus* Wagner, 1863 recovered from the same stratigraphic layer as the Ichthyosauria indet. specimen from Les Ardilles (Kimmeridgian,

https://doi.org/10.1017/pab.2025.2 Published online by Cambridge University Press

Table 1. Summary of information from Ichthyosauria, Plesiosauria, and Metriorhynchidae specimens sampled.

	Collection number	Museum/ institution	Taxonomy	Material	Estimated size (m)	Epoch	Stage	Locality	References
Ichthyosauria	-	Musée d'Histoire naturelle d'Auxerre (France)	Ichthyosauria indet.	Bones (36) and tooth (1)	6 to 8	Late Jurassic	Kimmeridgian	Les Ardilles, Auxerre, France	Mazin and Pavy (1995)
	PMO 222.655	Natural History Museum of Oslo (Norway)	*Keilhauia nui*	Bones (24)	2 to 3	Lower Cretaceous	Ryazanian	Slottsmøya Member, Spitsberg, Svalbard, Norway	Delsett et al. (2017)
	PMO 222.667	Natural History Museum of Oslo (Norway)	*Keilhauia* sp.	Bones (22) and teeth (3)	?	Late Jurassic	Volgian	Slottsmøya Member, Spitsberg, Svalbard, Norway	Delsett et al. (2019)
	PMO 222.669	Natural History Museum of Oslo (Norway)	*Palvennia hoybergeti*	Bones (25) and teeth (4)	?	Late Jurassic	Volgian	Slottsmøya Member, Spitsberg, Svalbard, Norway	Delsett et al. (2018)
Plesiosauria	PMO 212.662	Natural History Museum of Oslo (Norway)	Cryptoclididae indet.	Bones (38)	?	Late Jurassic	Volgian	Slottsmøya Member, Spitsberg, Svalbard, Norway	Under study
	PMO 222.663	Natural History Museum of Oslo (Norway)	*Colymbosaurus svalbardensis*	Bones (41)	?	Late Jurassic	Volgian	Slottsmøya Member, Spitsberg, Svalbard, Norway	Roberts et al. (2017)
	MHNLM.2005.16.1	Musée d'histoire Naturelle Le Mans (France)	Elasmosauridae indet.	Bones (22)	3.5 to 4	Middle Jurassic	Aalenian	Tessé Sandstones, Saint-Rémy du Val commune, Sarthe Department, France	Vincent et al. (2007)
Metriorhynchidae	MPV 2010.3.610	Paléospace Museum (France)	*Metriorhynchus* aff. *superciliosus*	Bones (20)	2	Middle Jurassic	Late Callovian	Marnes de Dives, Les Vaches Noires Cliffs, Villers-sur-Mer, France	Le Mort et al. (2022)
	-	Paléospace Museum (France)	Metriorhynchidae indet.	Teeth (2), probably from two specimens	?	Middle Jurassic	Late Callovian	Marnes de Dives, Les Vaches Noires Cliffs, Villers-sur-Mer, France	This study

Auxerre, France) to determine the oceanic paleotemperature of this deposit. Overall preservation and appearance of the studied specimens vary between the localities. The Ichthyosauria indet. specimen from Les Ardilles (France) is slightly deformed and marked by numerous fractures secondarily filled with calcite (Mazin and Pavy 1995). The skeletal remains of the specimen of *Metriorhynchus* aff. *superciliosus* from Les Vaches Noires Cliffs (France) seem to have been little affected by compaction, except for the skull, which shows a few cracks with surface recrystallization (Le Mort et al. 2022). The ichthyosaurs (PMO 222.655, PMO 222.667, PMO 222.669) and plesiosaurs (PMO 212.662, PMO 222.663) from the Slottsmøya Member (Spitsbergen) are partly eroded, probably by the action of suspended particles and sediments transported by bottom currents (Martill 1985; Reisdorf et al. 2012) and show recrystallizations of calcite and barite in the pores of the skeletal elements (Kihle et al. 2012; Delsett et al. 2016). The skeletal remains are also for the most part highly fractured, partly due to local faults within the deposit and to frost weathering. For instance, the specimen of *Keilhauia nui* (PMO 222.655) was crossed by large fractures (Delsett et al. 2017). Its skeletal elements are particularly fractured and have a sandy appearance.

Sampling Method

Approximately 40 mg of each skeletal element and tooth were ground to fine powder using a Dremel micro-drill equipped with a diamond-studded drill bit; cortical bone was selected to maximize the chances of preserving a biological isotopic record. Skeletal elements of complete and subcomplete specimens were grouped in five categories, as follows: "Skull" groups all the bone forming the skull and the mandible; "Cervical region" groups the cervical vertebra only in Plesiosauria; "Dorsal region" groups the dorsal vertebrae, ribs, and skeletal elements forming the pectoral and pelvic girdles; "Caudal region" groups the caudal vertebrae; and "Appendicular region" groups the humerus, femur, radius, ulna, tibia, fibula, metacarpals, metatarsals, phalanges, and accessory bone elements located in the limbs. For the specimen of *Colymbosaurus svalbardensis* (PMO 222.663), the "Appendicular region" was split into anterior right limb (ARL), anterior left limb (ALL), posterior right limb (PRL), and posterior left limb (PLL), as most of the elements were found in articulation (Delsett et al. 2016). For Ichthyosauria and *Metriorhynchus* aff. *superciliosus* specimens, cervical vertebrae were included in the "Dorsal region." A total of 247 skeletal elements and teeth were sampled, averaging about 20 and 40 samples per specimen. In addition to the bone and tooth samples, a sample of the recrystallization mineral observed in one dorsal vertebra from the Ichthyosauria indet. specimen from Les Ardilles was taken.

Bioapatite P_2O_5 Content and Phosphate Group Oxygen Isotope Analysis

Cortical bone and tooth powders ($n = 247$) were prepared using the wet chemical procedure detailed by Crowson et al. (1991) and modified by Lécuyer et al. (1993), which involves the isolation of phosphate ions (PO_4^{3-}) from the bioapatite, which are then precipitated as silver phosphate crystals (Ag_3PO_4). For each sample, 20–30 mg of cortical bone or tooth enamel powder was dissolved in 2 ml of 2M HF. The CaF_2 residue was separated by centrifugation, and the solution was neutralized by adding 2.2 ml of 2M KOH. Amberlite IRN78 anion-exchange resin beads were added to the solution to isolate the PO_4^{3-} ions. After 24 h, the solution was removed, and the resin was rinsed with deionized water and eluted with 27.5 ml of 0.5M NH_4NO_3. After 4 h, the Amberlite IRN78 anion-exchange resin beads were removed from the solution. Then, 0.5 ml of NH_4OH and 15 ml of an ammoniacal solution of $AgNO_3$ were added, and the solutions were placed in a thermostatted bath at 70°C for 7 h, allowing the slow and quantitative precipitation of Ag_3PO_4 crystals. The Ag_3PO_4 crystals were filtered, dried, and cleaned. For each sample, the P_2O_5 content, a proxy for qualitatively estimating the dissolution of phosphate minerals of the mineralized skeletal elements bioapatite in fossil specimens (Nemliher et al. 2004), was estimated. It was calculated from the recovered mass of silver phosphate (Ag_3PO_4) after the chemical purification of the samples and phosphate chemical yields obtained for the NIST SRM 120c standards (P_2O_5 = 33.34 wt%), assuming stoichiometric conversion of bioapatite phosphate ions into silver phosphate (Lécuyer et al. 2003).

For oxygen isotope composition measurements, five aliquots of 300 ± 20 µg of Ag_3PO_4 for each sample were mixed with 400 ± 50 µg of graphite in silver foil capsules. Oxygen isotope ratios were measured using a high-temperature vario PYRO cube elemental analyzer (EA), equipped with "purge and trap" technology (Fourel et al. 2011) and interfaced in continuous-flow mode to an IsoPrime isotope ratio mass spectrometer (Elementar UK, Cheadle, U.K.). To calibrate the measurements, the NBS 127 (barium sulfate precipitated from seawater from Monterey Bay, Calif., U.S.A., Sigma-Aldrich), and a silver phosphate precipitated from the international standards NIST SRM 120c (natural Miocene phosphorite from Florida, U.S.A., National Bureau of Standards) were used. The $\delta^{18}O$ value for NBS 127 is fixed to the certified value of +9.3‰ Vienna Standard Mean Ocean Water (VSMOW; Hut 1987; Halas and Szaran 2001) and that for NIST SRM 120c to +21.7‰ VSMOW according to Lécuyer et al. (1993), Chenery et al. (2010), and Halas et al. (2011) for correction of instrumental mass fractionation during CO isotope analysis. Along with the silver phosphate samples derived from bone and tooth bioapatite, silver phosphates precipitated from standard NIST SRM 120c were repeatedly analyzed ($\delta^{18}O_p$ = 21.7 ± 0.3‰, n = 59) to ensure that no isotope fractionation occurred during the wet chemistry. Values are reported as delta per mille values expressed with respect to VSMOW.

Oxygen and Carbon Isotope Analysis of Bioapatite Carbonate and Carbonate Content

Bone and tooth powders ($n = 71$) were pretreated to measure the oxygen and carbon isotope compositions of the carbonate group of the bone bioapatite (Plesiosauria: n = 40; Ichthyosauria: n = 29, *Metriorhynchus* aff. *superciliosus*: n = 1; and pachycormid fish tooth of *Hypsocormus* sp.: n = 1). The protocol used was that of Koch et al. (1997) and consisted of removing organic matter through a chemical reaction between bone powder and 0.4 ml of 2% sodium hypochlorite (NaOCl) for 24 h (0.4 ml NaClO per 10 mg of bone powder). The solution was centrifuged and rinsed three times with ultrapure water before 0.1 M acetic acid (CH_3COOH) was added for 24 h to remove any secondary carbonates that may have precipitated during the organic removal procedure. The solution was again centrifuged and rinsed three times. Then, the powders were dried at 50°C for 48 h before being collected. For each sample, three replicates of 2 mg were weighed into 3.7 ml round-bottomed glass vials and sealed (Exetainer, LABCO UK, Lampeter, Wales, U.K.). Oxygen ($\delta^{18}O_c$) and carbon ($\delta^{13}C_c$) isotope composition of the carbonate group of bone and tooth bioapatite was

https://doi.org/10.1017/pab.2025.2 Published online by Cambridge University Press

measured using an isoFLOW-type preparation system (Elementar GmbH, Germany) connected in continuous flow to a precisION isotope ratio mass spectrometer (Elementar UK). Each of the pretreated samples was reacted with saturated anhydrous phosphoric acid (H_3PO_4) prepared according to the protocol of McCrea (1950). The reaction took place at a constant temperature of 90°C. The CO_2 generated during acid digestion of the carbonate sample was then transferred to the mass spectrometer. Carbonate content (CO_3^{2-} %wt) of the bioapatite samples was measured based on the peak area of CO_2 detected by the mass spectrometer. Isotope measurements were corrected for instrumental drift and calibrated using two calcite isotopic standards: a Carrara marble (laboratory standard) with values of $\delta^{18}O_{VPDB}$ = −1.84‰ and $\delta^{13}C_{VPDB}$ = +2.03‰ (Fourel et al. 2015) and the NBS18 (international standard), whose values are $\delta^{18}O_{VPDB}$ = −23.2‰ and $\delta^{13}C_{VPDB}$ = −5.01‰ (Friedman et al. 1982; Hut 1987; Coplen et al. 2006); as well as NIST SRM 120c, whose values are $\delta^{18}O_{VPDB}$= −1.13‰ and $\delta^{13}C_{VPDB}$ = −6.27‰ (Passey et al. 2007). For bone and tooth apatite, the acid fractionation factor α(CO_2–apatite carbonate) of 1.00773 determined for the NIST SRM 120c phosphate rock reference material was selected (Passey et al. 2007). Values are reported as delta per mille values expressed with respect to VSMOW for oxygen and Vienna Pee Dee Belemnite (VPDB) for carbon.

Raman Spectroscopy

Characterization of the mineralogical composition of the samples was carried out using an XploRA Raman microscope equipped with a diode-pumped Nd:YAG laser at 532 nm. For each sample analyzed (n = 84), 10 spectra of 10 s were acquired at 100× magnification. The scattered light was detected in the range of 150 and 2000 cm^{-1}. The first-order band of a pure silicon reference material at 520.7 cm^{-1} was used to calibrate the spectrometer before each measurement. The full width at half maximum (FWHM) and the position of the ν1(PO_4^{3-}) fully symmetric stretching band were measured to obtain information on the mineralogical composition and crystal structure of bioapatite (Pucéat et al. 2004; Thomas et al. 2007, 2011; Dal Sasso et al. 2018; Barthel et al. 2020; Kral et al. 2022).

Body Temperature Estimates

Body temperatures of Ichthyosauria, Plesiosauria, and Metriorhynchidae were re-estimated from published tooth $\delta^{18}O_p$ values (Anderson et al. 1994; Bernard et al. 2010; Séon et al. 2020) as well as newly measured values from two teeth belonging to specimens of Metriorhynchidae indet. from Les Vaches Noires Cliffs (late Callovian, Villers-sur-Mer, France) and the teeth from the three specimens of ichthyosaur referred to as *Palvennia hoybergeti* (PMO 222.669), *Keilhauia* sp. (PMO 222.667), and Ichthyosauria indet. from Les Ardilles. The equation published by Lécuyer et al. (2013), adapted for air-breathing vertebrates, was used and an average ^{18}O-enrichment of +0.8 ± 0.9‰, for air-breathing fully aquatic marine vertebrates was applied (Séon et al. 2023). Paleolatitudes were reconstructed using the software developed by van Hinsbergen et al. (2015) and then used for the estimation of the $\delta^{18}O_{sw}$ values from the equation published by Alberti et al. (2020). For each locality, sea-surface temperature was calculated from the $\delta^{18}O_p$ values of contemporary fish using the equation of Lécuyer et al. (2013), considering that body temperature (T_b) is equal to seawater temperature (T_{sw}), and that $\delta^{18}O_{bw} \approx \delta^{18}O_{sw}$ (Kolodny et al. 1983). The associated error in temperature calculation is equal to 3°C (based on the slope of 4.5 of the Lécuyer et al. [2013] equation used). As no contemporary fish tooth has been analyzed for the Slottsmøya Member fossil locality, the environmental temperature was estimated from the oxygen isotope composition of one brachiopod shell from Hammer et al. (2011) using the oxygen isotope fractionation equation provided by Letulle et al. (2023).

Statistical Analyses

We used descriptive statistics to explore body temperature re-estimates and intraskeletal $\delta^{18}O_p$ variations in Mesozoic marine reptiles. The normality and homoscedasticity (the uniformity of the error associated with the variance for each of the values) of the $\delta^{18}O_p$ values could not be verified. Considering the variable number of samples for each set (between 1 and 14 samples), the nonparametric Mann-Whitney-Wilcoxon test was used to compare median values between two sets of observations, each corresponding to a skeletal region. Statistical tests were performed using R software with a significance threshold set at p-value < 0.05. Pearson's correlation coefficient r was employed to ascertain the degree of correlation between two quantitative variables.

Results

Bioapatite P_2O_5 Content and Phosphate Oxygen Isotope Composition ($\delta^{18}O_p$)

A total of 218 $\delta^{18}O_p$ values were acquired from 4 ichthyosaurs, 3 plesiosaurs, and 1 *Metriorhynchus* aff. *superciliosus* specimen in order to map regional heterothermies and reassess body temperatures. Almost all samples from each specimen could be analyzed, except a few samples that failed to yield silver phosphate after wet chemistry preparation, especially from the specimen of *Keilhauia nui* (PMO 222.655). P_2O_5 content expressed in weight percentage (wt%) and measured oxygen isotope composition from the phosphate group of each bone and tooth of all the specimens are reported in Supplementary Table 1 and synthetized in Table 2. P_2O_5 content for all specimens ranged from 2.0% to 40.5% (Table 2), with more than 90% of the values ranging from 15.3% to 40.5%. These results are consistent with the $\%P_2O_5$ measured for the skeletal and dental remains of modern marine vertebrates (26.0 ± 4.4%, range: [15.3, 33.92], n = 27; Nemliher et al. 2004). No significant differences were observed between the fossil deposits (Supplementary Figure 1A) or between specimens if we exclude the *Keilhauia nui* specimen (PMO 222.655), for which the percentage of P_2O_5 is significantly lower (Mann-Whitney-Wilcoxon test, p-value < 0.001; Supplementary Figure 1B). Globally, there are no significant differences in P_2O_5 content along the skeletal region, except for the Ichthyosauria indet. and *Colymbosaurus svalbardensis* specimens (Mann-Whitney-Wilcoxon test, p-value < 0.05; Supplementary Figure 2). Finally, no strong relationship between P_2O_5 content and $\delta^{18}O_p$ values is observed in Ichthyosauria and in Plesiosauria specimens (Pearson correlation test, r = 0.32; Supplementary Figure 3).

The intraskeletal variability of $\delta^{18}O_p$ is illustrated in Figures 1, 2, and 3, respectively for Ichthyosauria, Plesiosauria, and Metriorhynchidae. The *Hypsocormus* tooth recovered from the same stratigraphic layer as the specimen of Ichthyosauria indet. from Les Ardilles yielded a $\delta^{18}O_p$ value of 18.1 ± 0.2‰, and the $\delta^{18}O_p$ values of the Metriorhynchidae teeth VN6 and VN7 equaled 21.4 ± 0.2‰ and 19.8 ± 0.2‰, respectively (Supplementary Table 2). Intraskeletal variability in $\delta^{18}O_p$ values was observed for all the specimens of Ichthyosauria, the specimen of *Kimmerosaurus* sp., and the specimen

https://doi.org/10.1017/pab.2025.2 Published online by Cambridge University Press

Table 2. Synthesis of isotopic values ($\delta^{18}O_p$, $\delta^{18}O_c$, $\delta^{13}C_c$) and CO_3^{2-} and P_2O_5 content (wt%) of the bone and tooth bioapatite of the specimens of Ichthyosauria, Plesiosauria, and Metriorhynchidae. Abbreviations: ARL, anterior right limb; ALL, anterior left limb; PRL, posterior right limb; and PLL posterior left limb.

		$\delta^{18}O_p$ (‰, VSMOW)				$\delta^{18}O_c$ (‰, VSMOW)				$\delta^{18}O_c$ (‰, VPDB)				$\delta^{13}C_c$ (‰, VPDB)				CO_3^{2-} (wt%)				P_2O_5 (wt%)			
		Range	Mean	SEM	*n*	Range	Mean	SEM	*n*	Range	Mean	SEM	*n*	Range	Mean	SEM	*n*	Range	Mean	SEM	*n*	Range	Mean	SEM	*n*
Ichthyosauria indet.	Global	16.1 to 20.2	18.2	0.8	36	24.10 to 28.30	26.34	1.17	21	–6.58 to –2.56	–4.45	1.13	21	–8.56 to –1.56	–5.79	2.68	21	2 to 24	9	6	21	14.8 to 34.6	23.7	5.3	37
	Teeth	18.3	-	-	1	28.3			1	–2.56	-	-	1	–8.18	-	-	1	2	-	-	1	15.9	-	-	1
	Skull	17.6 to 18.2	17.9	0.3	5	26.70 to 28.20	27.4	0.53	4	–4.08 to –2.61	–3.36	0.52	4	–8.46 to –4.16	–7.3	1.82	4	2 to 8	4	2	4	26.4 to 34.6	31.3	3	5
	Dorsal region	16.1 to 20.2	18.4	1.2	14	24.10 to 27.20	25.78	0.94	8	–6.58 to –3.62	–4.99	0.89	8	–8.56 to –1.56	–4.57	2.76	8	4 to 19	11	5	8	14.9 to 28.8	21.4	4.4	14
	Caudal region	17.4 to 19.4	17.8	0.8	5	25.1	25.1	0	2	–5.65	–5.65	0	2	–6.48 to –3.59	–5.04	1.45	2	7 to 13	10	3	2	14.8 to 26.2	19.9	3.8	5
	Appendicular	17.8 to 18.5	18.1	0.2	11	25.4 to 28.2	26.43	0.89	6	–5.38 to –2.63	–4.38	0.87	6	–8.54 to –1.65	–6.28	2.45	6	3 to 24	9	7	6	18.2 to 29.5	25.5	3	12
Palvennia hoybergeti (PMO 222.669)	Global	14.1 to 15.9	15.1	0.5	27	18.20 to 19.10	18.62	0.41	5	–12.37 to –11.43	–11.93	0.42	5	–10.6 to –7.88	–9.28	1.05	5	2 to 5	4	1	5	2.0 to 32.9	18.8	7.9	29
	Teeth	15.5 to 15.9	15.7	0.1	4	-	-	-	-													17.7 to 24.6	21.8	2.7	4
	Skull	14.1 to 15.2	14.7	0.6	2	18.30			1	–12.27			1	–9.89			1	8			1	15.0 to 32.9	23.9	8	2
	Dorsal region	14.4 to 15.8	15.2	0.5	11	18.20 to 19.10	18.77	0.4	3	–12.37 to –11.43	–11.79	0.42	3	–10.60 to –7.88	–9.06	1.14	3	2 to 5	4	1	3	5.1 to 28.0	20.7	7.1	11
	Appendicular	14.2 to 15.4	14.9	0.4	10	18.5			1	–12.03			1	–9.31			1	5			1	2.0 to 26.0	15.2	7.8	12
Keilhauia nui (PMO 222.655)	Global	13.1 to 15.7	14.8	0.9	7																	3.3 to 15.0	8	3.8	7
	Dorsal region	13.1 to 15.7	14.8	1.0	5																	3.3 to 15.0	8.3	4	5
	Caudal region	14.8	-	-	1																	8.5	-	-	1
	Appendicular	14.9	-	-	1																	6.1	-	-	1
Keilhauia sp. (PMO 222.667)	Global	11.8 to 15.1	14.0	0.8	25	17.51 to 18.37	17.92	0.35	3	–13.01 to –12.17	–12.61	0.34	3	–8.40 to –6.77	–7.74	0.7	3	2 to 5	3	1	3	9.7 to 40.5	21.9	8.5	25
	Teeth	14.7 to 15.1	14.9	0.2	3																	25.3 to 30.2	27.4	2.0	3
	Skull	13.7 to 14.2	14.0	0.3	2																	25.7 to 30.5	28.1	2.4	2
	Dorsal region	11.8 to 15.1	13.8	0.9	10	17.51 to 17.87	17.69	0.18	2	–13.01 to –12.66	–12.84	0.18	2	–8.40 to –8.05	–8.23	0.18	2	3 to 4	2	0	2	10.3 to 36.8	23	7.3	10
	Appendicular	13.4 to 15.1	14.0	0.5	10	18.37	-	-	1	–12.17	-	-	1	–6.77	-	-	1	5	-	-	1	9.7 to 40.5	17.9	9.6	10

(*Continued*)

Table 2. (*Continued*)

		$\delta^{18}O_p$ (‰, VSMOW)				$\delta^{18}O_c$ (‰, VSMOW)				$\delta^{18}O_c$ (‰, VPDB)				$\delta^{13}C_c$ (‰, VPDB)				CO_3^{2-} (wt%)				P_2O_5 (wt%)			
		Range	Mean	SEM	*n*	Range	Mean	SEM	*n*	Range	Mean	SEM	*n*	Range	Mean	SEM	*n*	Range	Mean	SEM	*n*	Range	Mean	SEM	*n*
Colymbosaurus svalbardensis (PMO 222.663)	Global	13.1 to 15.9	14.3	0.8	40	17.83 to 20.06	18.62	0.74	13	–12.7 to –10.48	–11.92	0.73	13	–10.01 to –7.71	–8.76	0.75	13	2 to 5	3	1	13	8.4 to 32.4	21.5	5.5	40
	Dorsal region	13.2 to 15.9	14.7	0.9	12	17.84 to 20.06	18.7	0.9	5	–12.69 to –10.48	–11.9	0.9	5	–10.01 to –8.80	–9.30	0.5	5	2 to 5	3	1	5	21.1 to 32.4	27	3.4	12
	Caudal region	13.5 to 14.4	13.8	0.4	5	19.32	-	-	1	–11.25	-	-	1	–9.27	-	-	1	2	-	-	1	15.5 to 19.7	17.7	1.5	5
	ALL	14.9	-	-	1	18.44	-	-	1	–12.05	-	-	1	–7.71	-	-	1	4	-	-	1	23.7	-	-	1
	ARL	14.2 to 15.7	14.9	0.6	5	19.36	-	-	1	–11.16	-	-	1	–8.22	-	-	1	2	-	-	1	14.9 to 23.4	19.9	3.9	5
	PLL	13.1 to 14.2	13.5	0.4	9																	8.4 to 28.8	18.2	6.4	9
	PRL	13.7 to 14.6	14.2	0.3	8	17.83 to 19.51	18.3	0.7	5	–12.70 to –11.07	–12.20	0.7	5	–9.49 to –7.92	–8.4	0.6	5	2 to 4	3	1	5	15.3 to 27.4	20.4	3.9	8
Cryptoclididae indet. (PMO 212.662)	Global	15.8 to 17.1	16.5	0.4	38	12.47 to 20.63	18.28	1.47	27	–17.83 to –9.92	–12.25	1.42	27	–14.68 to –9.21	–10.50	1.09	27	2 to 18	6	3	27	16.5 to 31.1	24.3	4.2	38
	Cervical region	15.8 to 17.0	16.4	0.4	12	16.2 to 19.2	18.1	0.9	11	–14.27 to –11.39	–12.4	0.8	11	–11.99 to –9.56	–10.50	0.8	11	2 to 9	5	2	11	16.5 to 30.2	25	4.7	12
	Dorsal region	15.9 to 17.0	16.5	0.3	16	12.47 to 19.1	18.07	1.9	12	–17.83 to –11.43	–12.40	1.8	12	–14.68 to –9.21	–10.60	1.4	12	4 to 18	6	3	12	18.3 to 31.1	25	4	16
	Appendicular	16.0 to 17.1	16.6	0.4	10	18.00 to 20.63	19.3	1.3	4	–12.57 to –9.92	–11.30	1.2	4	–10.73 to –9.56	–10.02	0.5	4	2 to 5	4	1	4	17.5 to 28.8	22.4	3.4	10
Elasmosauridae indet. (MHNLM. 2005.16.1)	Global	17.5 to 18.5	18.2	0.3	22																	3.5 to 32.8	25.3	6.1	22
	Cervical region	17.9 to 18.4	18.3	0.2	6																	15.8 to 28.9	23.8	4.7	6
	Dorsal region	17.5 to 18.1	18.1	0.3	7																	3.5 to 31.7	23.6	8.8	7
	Caudal region	17.6 to 18.5	18.1	0.3	7																	22.4 to 32.8	27.5	3.2	7
	Appendicular	18.3 to 18.5	18.4	0.1	2																	26.7 to 28.3	27.5	0.8	2
Metriorhynchus aff. *superciliosus* (MPV 2010.3.610)	Global	19.3 to 20.3	19.9	0.3	20																	17.7 to 33.0	25.6	3.7	20
	Skull	19.4 to 19.9	19.7	0.2	3																	24.2 to 25.9	24.9	0.9	3
	Dorsal region	19.3 to 20.3	19.9	0.3	12	27.3	-	-	1	–3.53	-	-	1	–8.22	-	-	1	5	-	-	1	17.7 to 33.0	25.7	4.4	12
	Caudal region	19.9 to 20.1	20.0	0.1	5																	22.1 to 28.9	25.7	3.1	5

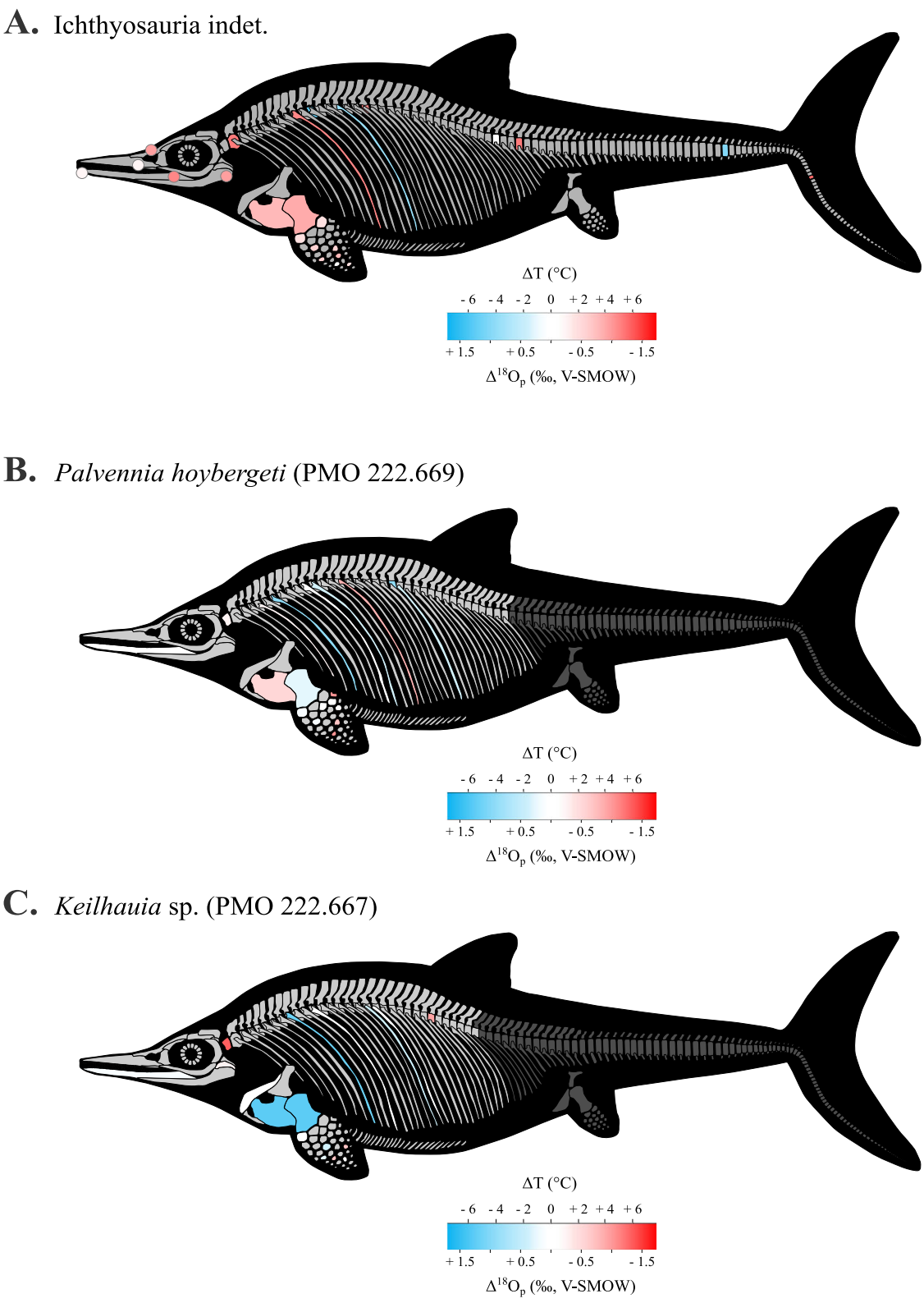

Figure 1. Regional heterothermies in ichthyosaurs. Phosphate oxygen isotope and temperature variability within the skeleton from **A,** the specimen of Ichthyosauria indet., **B,** the specimen of *Palvennia hoybergeti* (PMO 222.669), and **C,** the specimen of *Keilhauia* sp. (PMO 222.667). Color in bones corresponds to the $\delta^{18}O_p$ difference between bone and the midrange value, $(\delta^{18}O_{p\text{-}max} + \delta^{18}O_{p\text{-}min})/2$, of the skeleton. For paired skeletal elements, the mean value is illustrated. Available skeletal elements are shown in light gray, while unavailable elements and skeletal elements with potentially altered $\delta^{18}O_p$ values are shown in dark gray. Skeletal elements (e.g., "limb bones"; Supplementary Table 1) with precise location unknown are not illustrated, while the locations of vertebrae, ribs, and phalanges that have not been found in articulation have been established arbitrarily. The representation of the organisms is not to scale.

https://doi.org/10.1017/pab.2025.2 Published online by Cambridge University Press

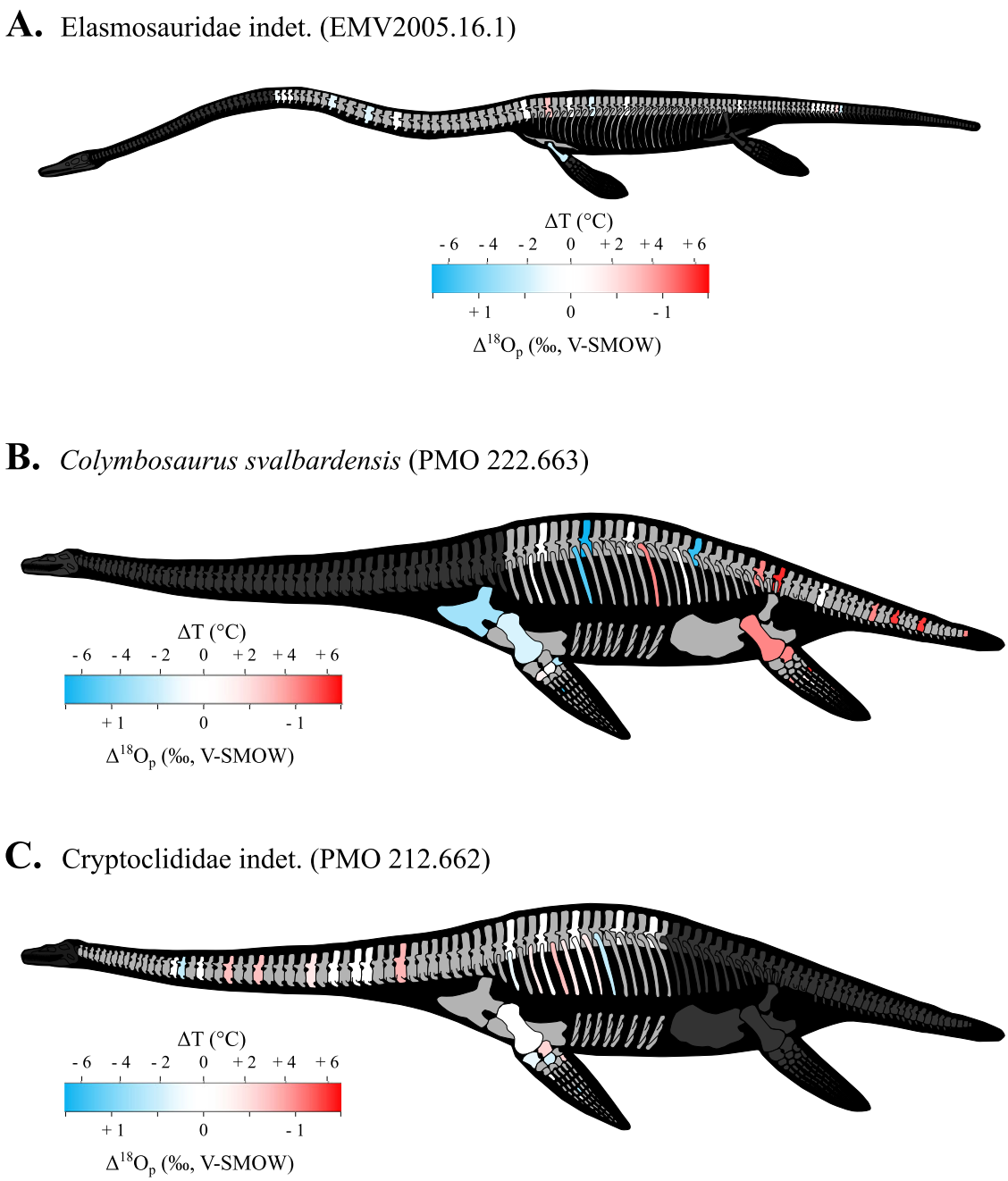

Figure 2. Regional heterothermies in plesiosaurs. Phosphate oxygen isotope and temperature variability within the skeleton from **A,** the specimen of Elasmosauridae indet. (MHNLM.2005.16.1), **B,** the specimen of *Colymbosaurus svalbardensis* (PMO 222.663), and **C,** the specimen of Cryptoclididae indet. (PMO 212.662). Color in bones corresponds to the $\delta^{18}O_p$ difference between bone and the midrange value, $(\delta^{18}O_{p\text{-}max} + \delta^{18}O_{p\text{-}min})/2$, of the skeleton. For paired skeletal elements, the mean value is illustrated. Available skeletal elements are shown in light gray, while unavailable elements and skeletal elements with potentially altered $\delta^{18}O_p$ values are shown in dark gray. Skeletal elements (e.g., "limb bones"; Supplementary Table 1) with precise location unknown are not illustrated, while the location of vertebrae, ribs, and phalanges that have not been found in articulation have been established arbitrarily. The representation of the specimens is not to scale.

of *Metriorhynchus* aff. *superciliosus*, but these differences are not significant between body regions (Mann-Whitney-Wilcoxon test, *p*-value > 0.05; Fig. 4). However, a trend seems to emerge in specimen PMO 222.667 of *Keilhauia* sp. and *Palvennia hoybergeti* specimen PMO 222.669, in which the teeth have overall higher $\delta^{18}O_p$ values than those of the bones, but the statistical significance of this observation could not be tested because of the small number of samples for each set ($n < 5$ for teeth). The only significant differences in $\delta^{18}O_p$ values along body regions observed are in the *Colymbosaurus svalbardensis* (PMO 222.663) specimen. Mann-Whitney-Wilcoxon statistical test results (p-value < 0.05; Fig. 4) clearly indicate that skeletal elements in the anterior part of the skeleton (dorsal vertebrae, ribs, left and right forelimbs) have significantly higher $\delta^{18}O_p$ values than skeletal elements in the posterior part (left and right hindlimbs and caudal vertebrae).

Plesiosaur specimens (*Colymbosaurus svalbardensis*, Cryptoclididae indet.) have been recovered in articulation (Vincent et al. 2007; Delsett et al. 2016); consequently, the relation between $\delta^{18}O_p$ values and distance from the trunk was investigated (Fig. 5A). No relationship between $\delta^{18}O_p$ values and position in the limbs

https://doi.org/10.1017/pab.2025.2 Published online by Cambridge University Press

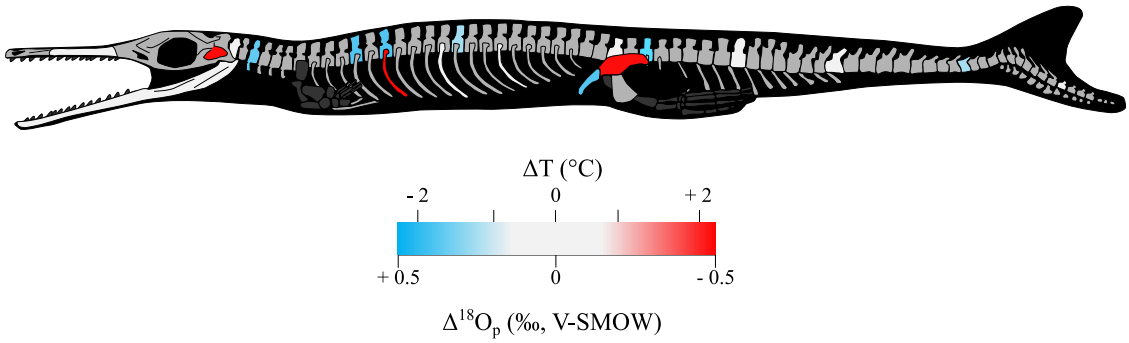

Figure 3. Regional heterothermies in *Metriorhynchus* aff. *superciliosus.* Phosphate oxygen isotope and temperature variability within the skeleton from the specimen of *Metriorhynchus* aff. *superciliosus* (MPV 2010.3.610). Color in bones corresponds to the $\delta^{18}O_p$ difference between bone and the midrange value, $(\delta^{18}O_{p\text{-}max} + \delta^{18}O_{p\text{-}min})/2$, of the skeleton. When both vertebrae centra and neural spine were measured, the mean value is illustrated. Available skeletal elements are shown in light gray, while unavailable elements are shown in dark gray. The representation of the specimen is not to scale.

(*Colymbosaurus svalbardensis*, Cryptoclididae indet.) or for the vertebral position in the neck (Cryptoclididae indet., Elasmosauridae indet.) was observed (Fig. 5B). To summarize, phosphate oxygen isotope compositions reveal variations for all studied Mesozoic marine reptiles (from 1.0‰ to 4.1‰), comparable to those observed in present-day marine vertebrates (from 1.5‰ to 2.8‰; Séon et al. 2022), and for most there are no significant differences in $\delta^{18}O_p$ from the individual skeletal regions.

Carbonate Bioapatite Oxygen and Carbon Isotope Compositions ($\delta^{18}O_c$ and $\delta^{13}C_c$) and Carbonate Content (wt%)

Oxygen and carbon isotope compositions of the carbonate group of bioapatite as well as carbonate content were measured to assess the preservation of the oxygen isotope composition of the phosphate group. All the values are reported in Supplementary Table 1, a synthesis is provided in Table 2 for each specimen, with a graphical representation in Figure 6. The tooth from the pachycormid fish *Hypsocormus* sp. recovered from the same stratigraphic layer as the specimen of Ichthyosauria indet. yielded a $\delta^{18}O_c$ value equal to 27.30 ± 0.20‰ (VSMOW), a $\delta^{13}C_c$ value equal to −4.27 ± 0.15‰ (VPDB), and a carbonate content of 4%. The $\delta^{18}O_c$ of calcite recrystallization sampled in the dorsal vertebra of the specimen of Ichthyosauria indet. from Les Ardilles is equal to 24.20 ± 0.10‰ (VSMOW) and to −0.10 ± 0.10‰ (VPDB) for $\delta^{13}C_c$.

Mineralogical Characteristics of Bones and Teeth from Mesozoic Marine Reptiles

Raman spectroscopy was used to assess possible mineralogical changes associated with fossilization and diagenetic processes. The Raman spectral parameters from ichthyosaurian and plesiosaurian bone elements and teeth are reported in Supplementary Table 3 and illustrated in Figure 7. The values of position of the ν1 (PO_4^{3-}) stretching band range from 939.6 cm^{-1} to 1023.4 cm^{-1}, whereas FWHM values range from 8.2 cm^{-1} to 34.7 cm^{-1} (Supplementary Table 3). No significant differences in ν1(PO_4^{3-}) stretching band values between individuals is observed (Mann-Whitney-Wilcoxon statistical test, *p*-value > 0.05), although some skeletal elements of the specimen of *Keilhauia nui* appear to have higher values. The Raman results indicate that there is little mineralogical change in the skeletal elements, except for some bone elements belonging to the *Keilhauia nui*, the *Keilhauia* sp., and the *Colymbosaurus svalbardensis* specimens.

Ichthyosauria, Plesiosauria, and Metriorhynchidae Body Temperature

Ichthyosauria, Plesiosauria, and Metriorhynchidae body temperature estimates were compared to environmental paleotemperatures, which range from 14 ± 2°C (Slottsmøya Member, Spitsberg, 65.5°N) to 34 ± 1°C (Les Ardilles, France, 34.5°N; Supplementary Table 2). Ichthyosauria, Plesiosauria, and Metriorhynchidae body temperature estimates are available in Supplementary Table 2 and reported against corresponding sea-water temperature estimates in Figure 8.

Our estimates indicate that ichthyosaurs had body temperatures ranging from 31°C to 45°C, close to extant Cetacea (Morrison 1962; Hampton et al. 1971; Yeates and Houser 2008; Fig. 8A) and systematically higher than those of the seawater in which they lived (between 3°C and 31°C higher; Supplementary Table 2). No relationship is observed between Ichthyosauria body temperatures and environmental oceanic temperatures (Pearson correlation test, $r = 0.3$; Fig. 8A). Plesiosauria body temperature range from 27°C to 34°C; these estimates are, as for Ichthyosauria, higher than those of their environment (between 5°C and 11°C; Supplementary Table 2) and correlate moderately with environmental temperatures (Pearson correlation test, $r = 0.42$; Fig. 8B). The estimated body temperatures of Metriorhynchidae, ranging from 25°C to 32°C, are 3°C to 5°C higher than environmental temperatures (Supplementary Table 2), while being highly correlated (Pearson correlation test, $r = 0.96$; Fig. 8C).

Discussion

Preservation of the Biological $\delta^{18}O_p$ Values

Before discussing the thermophysiological significance of the $\delta^{18}O_p$ values of bone and tooth bioapatite, pristine preservation of the isotope record needs to be assessed. Biotic and abiotic processes leading to the decomposition, burial, and fossilization of living organisms may alter the pristine isotope composition of bioapatite through processes of secondary precipitation, ion adsorption, or dissolution–recrystallization of bioapatite (Kolodny et al. 1996; Blake et al. 1997; Trueman et al. 2003; Zazzo et al. 2004a,b). Although no method can definitely demonstrate whether the original isotope compositions have been preserved, several ways to assess the preservation state of the oxygen isotope record have been proposed (Iacumin et al. 1996; Kolodny et al. 1996; Fricke et al. 1998; Lécuyer et al. 2003; Pucéat et al. 2004; Zazzo et al. 2004a,b;

https://doi.org/10.1017/pab.2025.2 Published online by Cambridge University Press

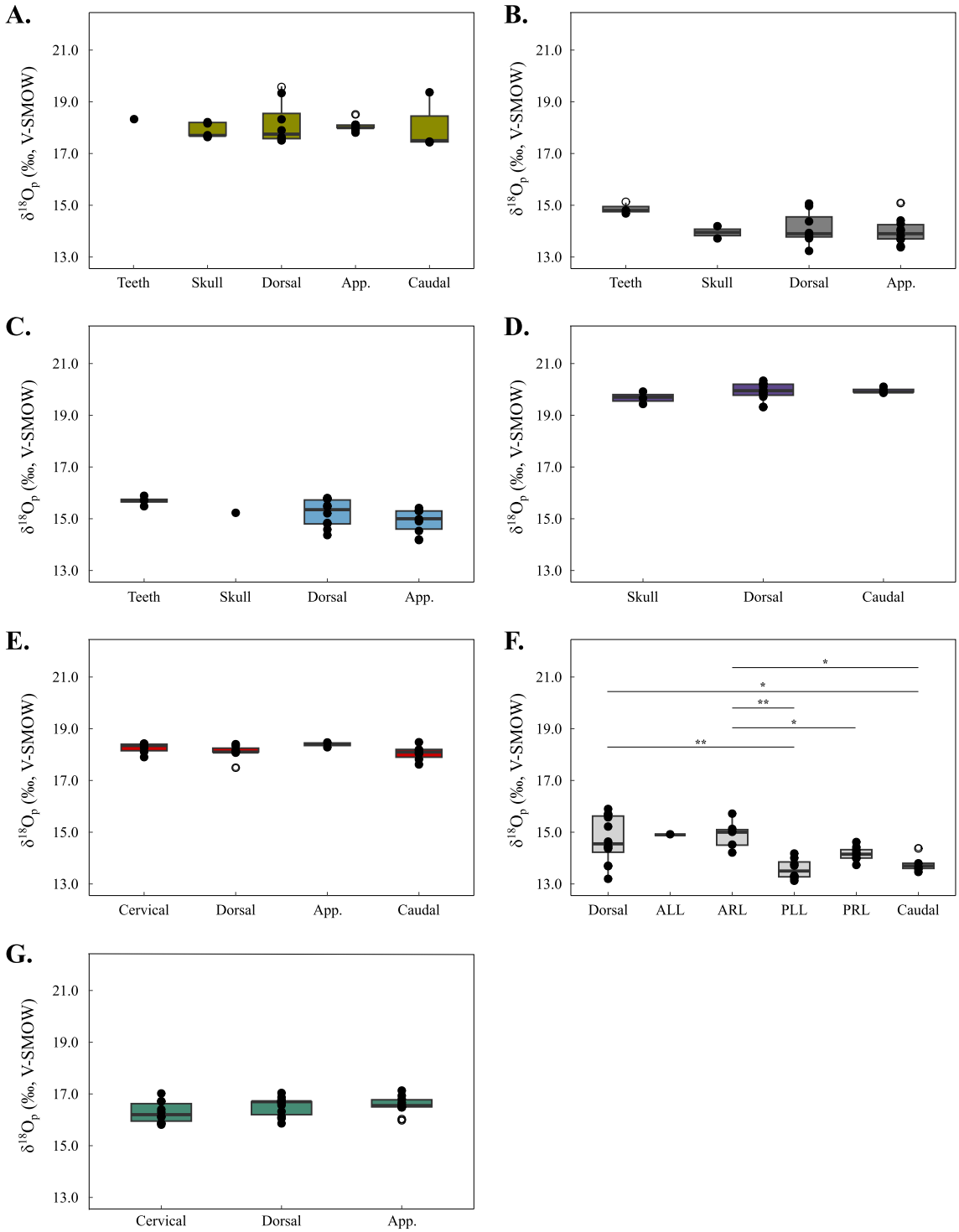

Figure 4. Box plots showing the $\delta^{18}O_p$ value distribution of bones sets for the specimens of Ichthyosauria (**A,** Ichthyosauria indet.; **B,** *Keilhauia* sp.; **C,** *Palvennia hoybergeti*), *Metriorhynchus* aff. *superciliosus* **(D)** and Plesiosauria (**E,** Elasmosauridae indet.; **F,** *Colymbosaurus svalbardensis*; and **G,** Cryptoclididae indet.). Asterisks indicate the significance of the observed differences between pair of groups: **p*-value < 0.05; ***p*-value < 0.01; ****p*-value < 0.001. Outliers are plotted as white circles. The horizontal bars in the boxes correspond to the medians and the whiskers to the minimum and maximum values. The average analytical error for each bone analyzed is on the order of 0.3‰. Abbreviations: App., Appendicular region; ALL, anterior left limb; ARL, anterior right limb; PLL, posterior left limb; PRL, posterior right limb.

Tütken et al. 2008; Keenan 2016; Lécuyer and Flandrois 2023; Turner-Walker et al. 2023).

In general, enamel is widely considered to be more resistant to diagenetic processes compared with bones (e.g., Lowenstam and Weiner 1989; Sillen and LeGeros 1991; Kohn et al. 1999; Lee-Thorp and Sponheimer 2003; Gehler et al. 2011), as it possesses a high crystallinity index, being composed of 95% bioapatite crystals. In addition, bioapatite crystals are larger and more compact than those in bone (Pasteris et al. 2008). As a result, the space between the crystals is reduced, limiting fluid circulation, interaction with

https://doi.org/10.1017/pab.2025.2 Published online by Cambridge University Press

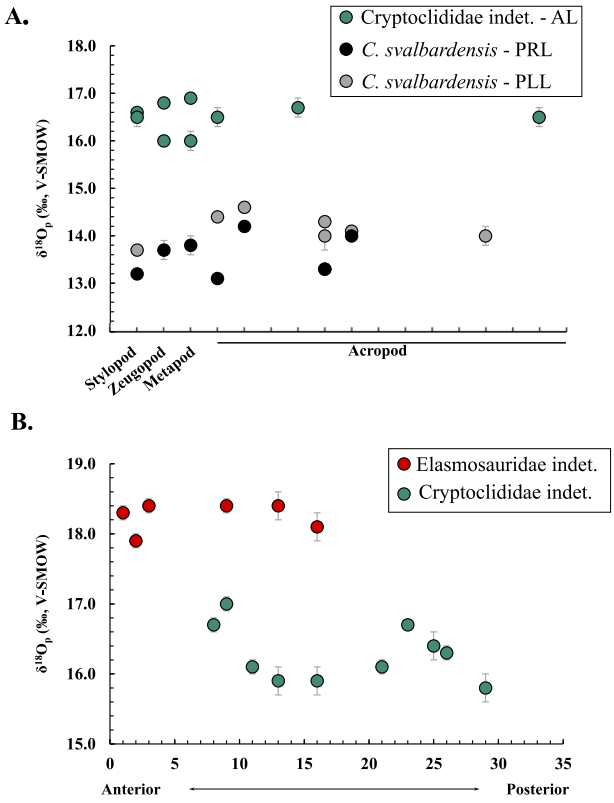

Figure 5. A, $\delta^{18}O_p$ values (‰, VSMOW) according to bone position within the limb for the specimen of Cryptoclididae indet. and the specimen of *Colymbosaurus svalbardensis*. Stylopod set corresponds to the femur or the humerus, Zeugopod set to radius and ulna or tibia and fibula, Metapod set to metacarpals or metatarsals, and Acropod set to phalanges. Abbreviations: AL, Anterior limb indet.; PRL, posterior right limb; PLL, posterior left limb. **B,** $\delta^{18}O_p$ values (‰, VSMOW) according to position of the vertebra within the cervical region for the specimen of Elasmosauridae indet. and the specimen of Cryptoclididae indet.

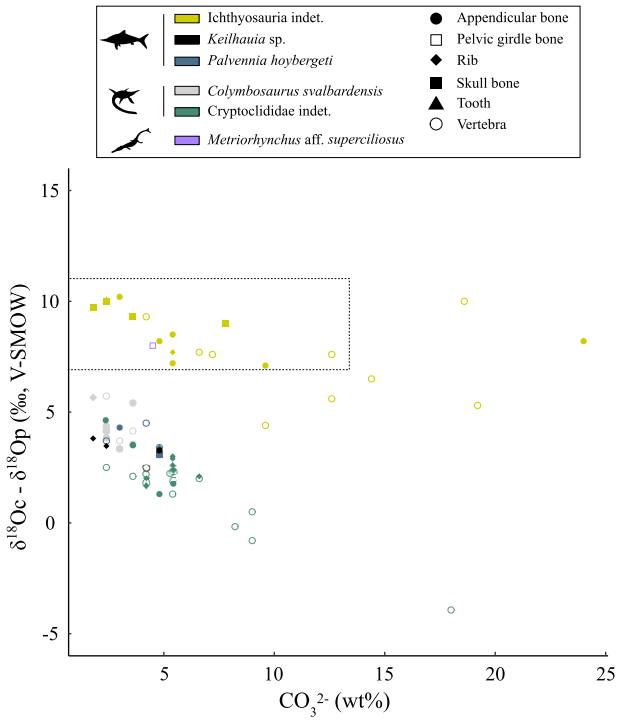

Figure 6. The $\delta^{18}O_c - \delta^{18}O_p$ differences between teeth and bone types plotted against carbonate content (wt%) of bioapatite. The dashed rectangle zone corresponds to the combination of parameters that would indicate a potential biological preservation of the oxygen isotope composition of the bioapatite of teeth and bones. Silhouettes were made by Gareth Monger for Ichthyosauria and Metriorhynchidae and T. Michael Keesey for Plesiosauria. Images downloaded from PhyloPic and used under a CCBY 3.0 license: https://creativecommons.org/licenses/by/3.0.

bacterial and microbial organisms, and precipitation of secondary minerals (LeGeros 1981; Driessens and Verbeeck 1990). The precipitation of secondary minerals leads to mineralogical changes observable through mineralogical characterization methods such as Raman spectroscopy. According to Thomas et al. (2007, 2011), bones and teeth altered by diagenetic processes have peak widths (FWHM) of $\nu1(PO_4^{3-})$ at half height of less than 9 cm^{-1} and band positions of $\nu1(PO_4^{3-})$ greater than 964.7 cm^{-1}. Among the analyzed samples, few skeletal elements have parameters that might suggest that they are mineralogically altered (Fig. 6), including different type of bones (skull bones, vertebrae, and phalanges) from specimens of *Palvennia hoybergeti*, *Keilhauia nui*, and *Colymbosaurus svalbardensis*. The sandy appearance of the remains from the *Keilhauia nui* specimen could explain why so few silver phosphate crystals were recovered at the end of the chemical preparation. Their low P_2O_5 content compared with the other specimens from the same stratigraphic layer and the mineralogical change observed by Raman spectroscopy would indicate the presence of bone alteration (Table 2, Supplementary Fig. 1B).

To assess the effect of diagenetic processes on the oxygen isotope composition of the bones and the teeth, we used the difference between oxygen isotope compositions of biogenic bioapatite phosphate and corresponding structural carbonate ($\delta^{18}O_c - \delta^{18}O_p$), the carbonate content (CO_3^{2-} %wt) of bioapatite, and the carbon isotope composition of bioapatite structural carbonate ($\delta^{13}C_c$) (Fig. 6). Samples that have either $\delta^{18}O_c - \delta^{18}O_p$ differences lower than +7‰ and higher than +11‰ (Iacumin et al. 1996; Pellegrini et al. 2011; Sisma-Ventura et al. 2019) or a carbonate content higher than +13.4% must be regarded with caution, as they may reflect a potential diagenetic alteration (Brudevold and Soremark 1967; Vennemann et al. 2001; McElderry et al. 2013; Wingender et al.

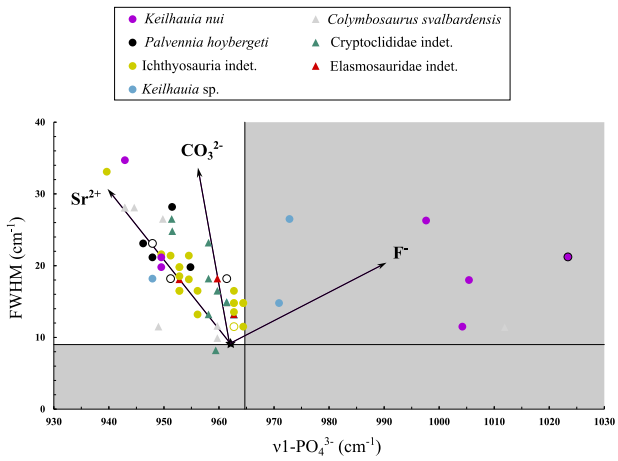

Figure 7. The $\nu1(PO_4^{3-})$ stretching band position and full width at half maximum (FWHM) measured for Ichthyosauria and Plesiosauria bones and teeth (Supplementary Table 3). Empty symbols represent enamel samples, while solid symbols represent bone samples. The gray zone corresponds to the combination of parameters that would indicate a mineralogical alteration of the bioapatite of teeth and bones. The black arrows indicate the evolution of the position of the $\nu1(PO_4^{3-})$ stretching band position and the FWHM depending on the type of ionic substitution within the bioapatite (Thomas et al. 2011).

https://doi.org/10.1017/pab.2025.2 Published online by Cambridge University Press

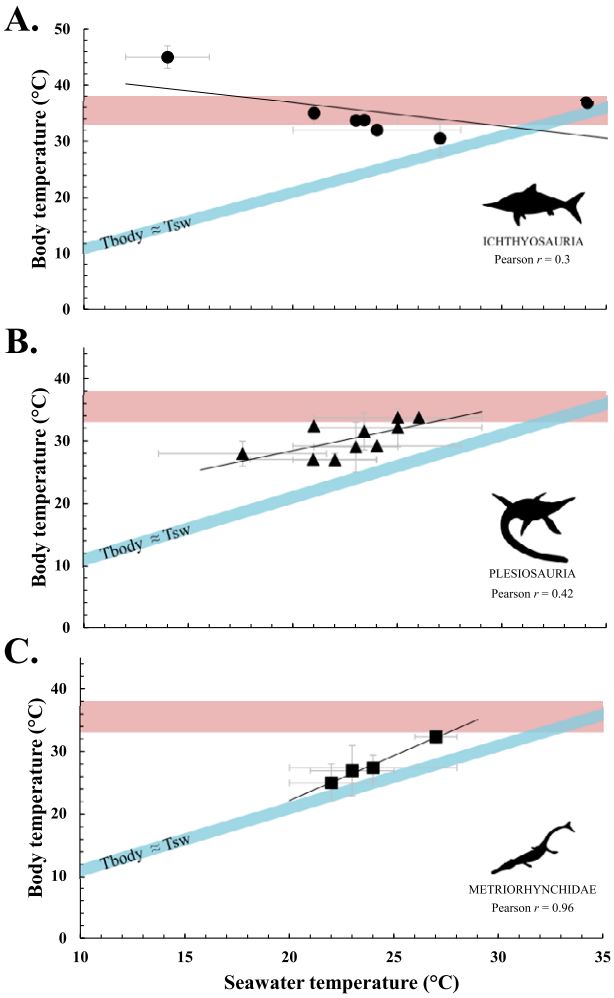

Figure 8. Body temperature estimates of Ichthyosauria **(A)**, Plesiosauria **(B)**, and Metriorhynchidae **(C)** from tooth enamel $\delta^{18}O_p$ values (new data in Supplementary Table 1 and published data in Supplementary Table 2) reported against environmental seawater temperature of their living environments. The body temperature range of extant homeothermic endotherm Cetacea is illustrated in red (Morrison 1962; Hampton et al. 1971; Yeates and Houser 2008), while the body temperature range shown in blue corresponds to the temperature range of a strictly ectothermic poikilothermic model organism whose body temperature is equal to the environmental temperature +2°C. Body and environmental temperatures were calculated using the equation of Lécuyer et al. (2013) and considering the latitudinal gradient of $\delta^{18}O_{sw}$ values of Alberti et al. (2020) and an ^{18}O-enrichment of body water relative to environmental water of +0.8 ± 0.9‰ for Mesozoic marine reptiles (Séon et al. 2023). Silhouettes were made by Gareth Monger for Ichthyosauria and Metriorhynchidae and T. Michael Keesey for Plesiosauria. Images downloaded from PhyloPic and used under a CCBY 3.0 license: https://creativecommons.org/licenses/by/3.0.

2021). All the samples from Ichthyosauria, Plesiosauria, and Metriorhynchidae have $\delta^{18}O_c - \delta^{18}O_p$ differences lower than the critical value of +11‰, but most of them are below +7‰. Nonetheless, some of them possess carbonate content greater than +13.4%, especially those from bones belonging to the specimen of Ichthyosauria indet. from Les Ardilles (Fig. 6), in line with the secondary calcite mineralization observed during sampling. Moreover, a trend is observed between carbonate contents and $\delta^{18}O_c$ values considering the tooth $\delta^{18}O_c$ value as the pristine biological signal and that of the secondary calcite mineralization, which would form the diagenetic end-member (Supplementary Fig. 4). This relationship also highlights the link between the occurrence of high carbonate content and the ultrastructure (e.g., connected porosity) of the bones, here the vertebrae, as among all the skeletal elements analyzed in the specimen of Ichthyosauria indet., six (n = 6) are vertebrae and two (n = 2) are limb bones. These skeletal elements are among the bones with the highest porosities within Ichthyosauria (Anderson et al. 2019).

Finally, most of the $\delta^{13}C_c$ values, when plotted against CO_3^{2-} (wt%), conform to two different mixing lines. In the specimen of Cryptoclididae indet. from Spitsbergen, the data point to variable amounts of secondary calcite with $\delta^{13}C_c$ values of −15‰ (Fig. 9), which indicates a ^{13}C-depleted organic carbon source typical of the sulfate reduction zone (Meister and Reyes 2019). In the specimen of Ichthyosauria indet., the data point to variable amounts of more ^{13}C-enriched secondary calcite with $\delta^{13}C_c$ values of ~0‰, in agreement with the value of −0.1‰ measured on intra-bone calcite sampled from the same specimen. These higher isotopic values could either reflect an early precipitation of calcium carbonate close to the sediment–seawater interface with a significant seawater influence or formation below the sulfate reduction zone close to a ^{13}C-enriched methanogenic CO_2 source (Meister and Reyes 2019). In both specimens, $\delta^{13}C_c$ values point to an almost identical, well-preserved end-member with low CO_3^{2-} contents (<10%) and $\delta^{13}C_c$ values of −8‰ to −10‰ VPDB dominated by structural bioapatite carbonates. The range of $\delta^{13}C_c$ values recorded for these CO_3^{2-}-poor samples of marine reptiles are identical to that previously reported for ancient air-breathing vertebrates (Séon et al. 2020), but substantially lower than the $\delta^{13}C_c$ values recorded in the pachycormid *Hypsocormus* sp. teeth measured from Les Ardilles and from coeval fossil fishes (−5.47‰ to +3.15‰ VPDB; Séon et al. 2020). As expected, air-breathing reptiles have lower $\delta^{13}C_c$ values than fish. In fact, the $\delta^{13}C$ values of air-breathing reptiles mainly reflect those of their diet, with isotopic fractionation depending on their digestive physiology (Passey et al. 2005). In fish, on the other hand, the $\delta^{13}C$ values of carbonate come from the diet, but also from the contribution of a large amount of dissolved inorganic carbon in the surrounding water (McConnaughey et al. 1997), which has a high $\delta^{13}C$ value (~0‰ to 2‰; Santos et al. 2011). These features demonstrate that, despite the different taphonomic history suggested by the diagenetic $\delta^{13}C_c$ values at the two sites, the geochemical signature of the CO_3^{2-}-poor samples is preserved and hence paleobiologically informative.

From here on, based on the evidence provided by mineralogical and isotope proxies, we assume that $\delta^{18}O_p$ values from most of the Ichthyosauria, Plesiosauria, and Metriorhynchidae samples, except the *Keilhauia nui* specimen (PMO 222.655), have kept at least a significant part of their original oxygen isotope compositions and might be interpreted in terms of thermophysiology. As a precaution, we removed all the skeletal elements for which doubt was expressed regarding the preservation of the original isotopic signal (mineralogical, carbonate content, and isotope clues; Supplementary Table 1).

Intraskeletal Body Temperature Distribution in Ichthyosauria, Plesiosauria, and Metriorhynchidae

The oxygen isotope composition of air-breathing aquatic tetrapods is controlled by their body temperatures, the proportion and isotopic composition of metabolic and drinking waters, and the breathing-induced isotope enrichment factor relative to these sources of waters. The possible occurrence of salt glands in at least some taxa of Metriorhynchidae (Fernández and Gasparini 2000, 2008; Gandola et al. 2006; Cowgill et al. 2023), Ichthyosauria (Wahl 2012; Campos et al. 2020; Massare et al. 2021), and Plesiosauria

https://doi.org/10.1017/pab.2025.2 Published online by Cambridge University Press

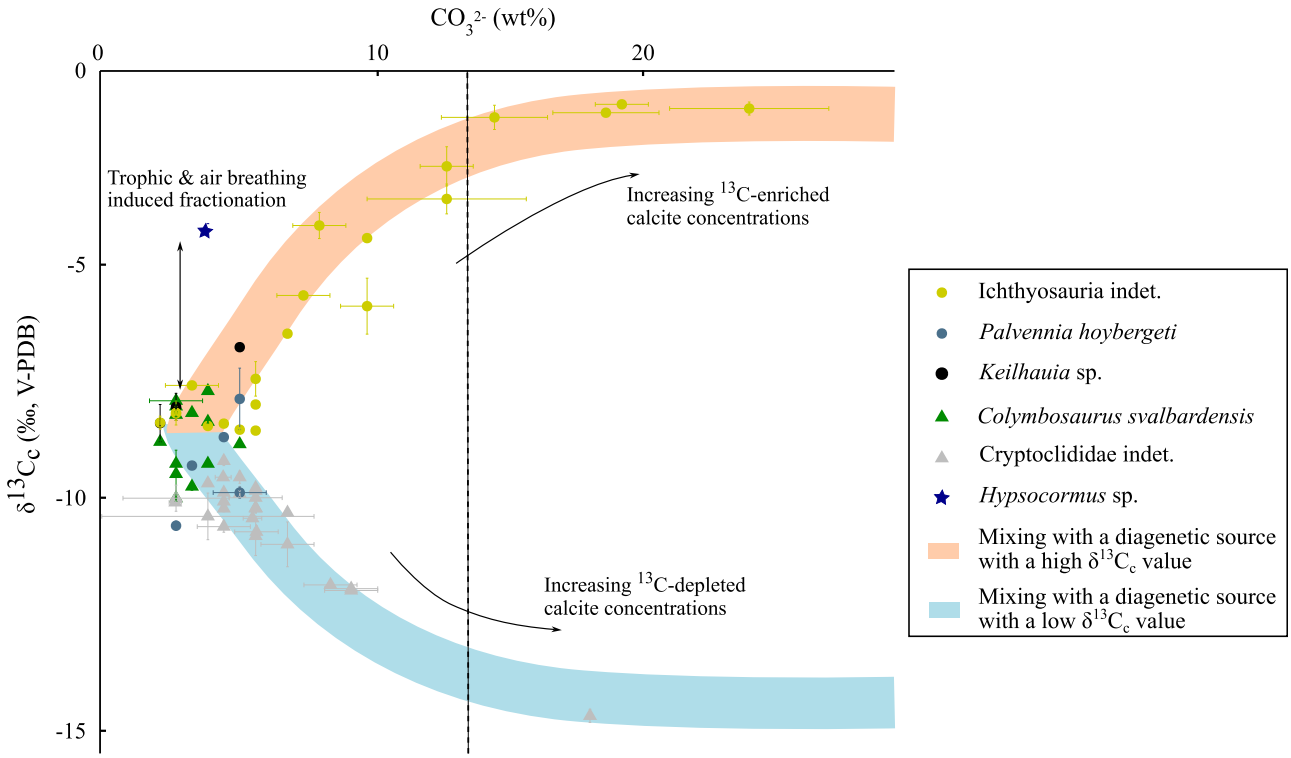

Figure 9. The $\delta^{13}C_c$ values (‰, VPDB) of bone elements and teeth in ichthyosaurs and plesiosaurs as a function of carbonate content (wt%). The values corresponding to the *Hypsocormus* sp. tooth found in the same stratigraphic layer as the Ichthyosauria indet. specimen are also plotted. The dotted line marks the boundary between mineralized elements with a carbonate content greater than or less than +13.4%.

(Buchy et al. 2006; O'Gorman and Gasparini 2013; Páramo-Fonseca et al. 2019) indicates that they would have been able to drink seawater to maintain their water balance. We thus consider that seawater was the main source of water and thus oxygen, as is the case in extant reptiles with salt glands (Rash and Lillywhite 2019). Because the $\delta^{18}O_{sw}$ value influencing $\delta^{18}O_p$ values can vary over time and specific regions, the timing of oxygen incorporation into the bone and tooth bioapatite needs to be identified to accurately compare the $\delta^{18}O_p$ values of different skeletal elements and identify potential regional heterothermies.

Similar to most reptiles, Ichthyosauria, Plesiosauria, and Metriorhynchidae continuously replaced their teeth. According to the studies conducted by Kear et al. (2017) and Maxwell et al. (2011a,b, 2012), the mineralization time for the teeth was estimated to be at most 2 to 3 years for plesiosaurs and approximately 1 year for ichthyosaurs. Although there is currently no available information regarding the tooth renewal time of Metriorhynchidae, it can be assumed that it was comparable to that of extant crocodylomorphs, which is approximately 3 to 15 months (Erickson 1996; Finger et al. 2019). In Ichthyosauria and Plesiosauria, bones underwent regular remodeling throughout life, as evidenced by studies conducted by Kolb et al. (2011), Delsett and Hurum (2012), Houssaye et al. (2014), and O'Keefe et al. (2019). For the Metriorhynchidae, cyclical growth marks in some bones indicate little bone remodeling and lack of or few secondary osteons (Hua and de Buffrénil 1996; de Buffrénil et al. 2021); thus, the time recorded in the bones is likely to be slightly longer. The $\delta^{18}O_p$ values of the teeth and bones of Ichthyosauria, Plesiosauria, and Metriorhynchidae can be compared, as these tissues record a period ranging from one to several years. Furthermore, the annual and seasonal fluctuations in modern $\delta^{18}O_{sw}$ values in the open ocean and the depositional environments in which the marine reptiles studied were discovered (Hammer et al. 2011; Lebrun and Courville 2013; Delsett et al. 2016) are typically only a few tenths of a per mille (~ ±0.5‰; LeGrande and Schmidt 2006), so this alone cannot fully explain the observed intraindividual $\delta^{18}O_p$ variations in ichthyosaurs and plesiosaurs of more than 1‰ to 3‰. Thus, we postulate that the $\delta^{18}O_p$ variability recorded in bones and teeth from the Ichthyosauria, Plesiosauria, and Metriorhynchidae studied mostly reflects temperature variations. Nevertheless, this supposition is contingent upon the absence of migration for these animals. It is possible that migrations between high and low latitudes, as well as between open-marine environments and restricted or brackish environments, may exert a considerable influence in intraskeletal $\delta^{18}O_p$ variability. A further limitation of this study is the lack of information available regarding the migratory patterns of these taxa, which precludes an investigation into this possibility.

Assuming that the temporal variation in the oxygen isotope composition of the body water of Ichthyosauria, Plesiosauria, and Metriorhynchidae is approximately constant over time, as was shown in modern vertebrates (cetaceans: Séon et al. 2023; sheep: Green et al. 2018), we can infer the range of mineralization temperatures across their bodies using the $\delta^{18}O_p$ values of the geochemically best-preserved skeletal elements. Thus, using the equation of Lécuyer et al. (2013), we obtain a mineralization temperature range of approximately 8°C to 12°C for Ichthyosauria (Fig. 1), 4°C to 12°C for Plesiosauria (Fig. 2), and on the order of 4°C to 5°C for *Metriorhynchus* aff. *superciliosus* (Fig. 3). In comparison, the mineralization temperature range of skeletal elements estimated from bone $\delta^{18}O_p$ is around 8°C to 12°C for extant homeothermic endotherms Cetacea and Pinnipedia, 10°C for poikilothermic endotherm Atlantic bluefin tuna, and 15°C for poikilothermic endotherm

https://doi.org/10.1017/pab.2025.2 Published online by Cambridge University Press

swordfish (Séon et al. 2022, 2024), while direct measurement of body temperature range for poikilothermic ectotherms such as crocodiles and turtles has been estimated to be ~10°C (Dunham et al. 1989; Markwick 1998). Note that for specimens of Elasmosauridae indet. and *Metriorhynchus* aff. *superciliosus*, we were unable to analyze distal skeletal elements belonging to the appendicular skeleton (not preserved), which may explain why the mineralization temperature ranges for these specimens are narrower than for the other analyzed taxa (Figs. 2, 3). For all specimens, the comparison between the different skeletal regions does not allow us to identify heterothermies in Mesozoic marine reptiles. Indeed, we did not observe the expected colder limbs and tails and differences in neck temperatures in Plesiosauria. This could, in part, be the result of a homogenization of the $\delta^{18}O_p$ values of bones, or at least a reduction in the original differences, by the various postmortem diagenetic processes and not detected by the methods used here (Raman spectroscopy, $\delta^{18}O_c - \delta^{18}O_p$ offset), as has been hypothesized previously by other authors who have studied the intraskeletal variations in the $\delta^{18}O$ of extinct organisms (Barrick and Showers 1994). Significant differences in $\delta^{18}O_p$ values of the dorsal region (vertebrae, ribs, girdle bones) and the limbs are only observed for the specimen of *Colymbosaurus svalbardensis* (Fig. 4). However, the differences observed are contrary to what we would have expected. This would indicate a higher average temperature of mineralization of the hindlimbs compared with the skeletal elements of the trunk (vertebrae, ribs, pectoral, and pelvic bones). In the specimen of *Colymbosaurus svalbardensis* (PMO 222.663), skeletal elements of the anterior region (dorsal vertebrae, ribs, left and right forelimbs) have significantly higher values than those of the posterior region (left and right hindlimbs and caudal vertebrae). These significant differences in $\delta^{18}O_p$ appear unusual in terms of thermoregulatory strategies and could be the result of a preservation difference between the more weathered anterior and posterior skeletal elements of the specimen (Delsett et al. 2016). Regarding the limbs of Plesiosauria, the osteo-histological study carried out by Delsett and Hurum (2012) on two specimens of *Colymbosaurus svalbardensis* (PMO 216.838, PMO 216.377) indicates that the most distal limb bone elements display growth striations, perhaps resulting from cyclic growth. In our study, our data reveal no clear relationship between $\delta^{18}O_p$ values and the position of the skeletal element within the limb (Fig. 5A). Thus, no body temperature gradient can be identified in the limb of Plesiosauria based on the geochemical approach. An identical conclusion can be drawn regarding the possible presence of a temperature gradient in the neck of Plesiosauria, as our detailed mapping of the cervical region shows no relationship between $\delta^{18}O_p$ and vertebral position (Fig. 5B). Finally, the only systematic trend recorded in our dataset concerns teeth, which, when analyzed alongside bones from the same organism, exhibit higher $\delta^{18}O_p$ values than the bones, including skull elements located close to the analyzed teeth in *Keilhauia* sp. specimen PMO 222.667 and *Palvennia hoybergeti* specimen PMO 222.669 (Fig. 4). Interestingly, similar observations have been made in odontocetes (Barrick et al. 1992; Séon et al. 2022), which would indicate that teeth mineralize at lower temperatures than skull bones (lack of insulating tissue on the rostrum). However, the number of teeth analyzed makes it impossible to determine whether these differences are significant or not. Furthermore, in the monophyodont odontocetes, there is the influence of lactation, which probably includes uncertainties in the interpretation of odontocete tooth $\delta^{18}O_p$ and makes them incomparable with Ichthyosauria. On the other hand, Séon et al. (2022) observed no $\delta^{18}O_p$ differences between teeth and skull bones in the polyphyodont Atlantic bluefin tuna. Differences in $\delta^{18}O_p$ values between teeth and bones in Ichthyosauria could be explained by a difference in mineralization temperature at the rostrum of about 3°C to 4°C, but the lower number of values available for each of these observation series means that we must be cautious about such considerations. Indeed, the observed higher values from the teeth could also result from differences in isotopic preservation between tooth enamel and bones.

Reassessment of Ichthyosauria, Plesiosauria, and Metriorhynchidae Body Temperature and Thermoregulatory Strategies

Previous isotope-based reconstructions of extinct marine reptile body temperatures opted for an ^{18}O-enrichment of body water relative to drinking water of +2‰ (Bernard et al. 2010; Séon et al. 2020; Leuzinger et al. 2023), originally estimated by Amiot et al. (2007) from body fluids of young Nile crocodiles (*Crocodylus niloticus*), and Barrick et al. (1999) for turtles (*Chrysemys* sp.). These species have a semiaquatic ecology, low body mass (1.2 kg to 5 kg), and relatively low metabolic rates. We therefore consider that a +2‰ enrichment of body water relative to environmental water may not be the most appropriate value for Mesozoic fully marine reptiles. We considered instead the +0.8 ± 0.9‰ enrichment value measured by Séon et al. (2023) for fully aquatic air-breathing vertebrates (*Orcinus orca* and *Tursiops truncatus*; 150 to 3600 kg), which appears more appropriate considering the ecology, the size, and the putative thermo-metabolism of the Ichthyosauria, Plesiosauria, and Metriorhynchidae studied here.

To reassess Ichthyosauria, Plesiosauria, and Metriorhynchidae body temperatures, we have favored the use of tooth enamel, as its robustness against diagenetic alteration has been demonstrated in previous studies (Lowenstam and Weiner 1989; Sillen and LeGeros 1991; Kohn et al. 1999; Lee-Thorp and Sponheimer 2003; Gehler et al. 2011). A last important change in our work relative to previous studies is the use of a spatially variable $\delta^{18}O_{sw}$ values calculated using the hemispheric gradient proposed by Alberti et al. (2020). This gradient places $\delta^{18}O_{sw}$ highest values in subtropical areas subject to high evaporation and lowest values in high-latitude seas receiving high fluvial input from surrounding large continental areas, consistent with both modeling (Zhou et al. 2008) and empirical evidence (Letulle et al. 2022). We thus consider this scenario as far more realistic than the $\delta^{18}O_{sw}$ hypothesis used previously (Bernard et al. 2010; Séon et al. 2020). Together, the use of revised values and spatial changes in $\delta^{18}O_{sw}$ values produce new body temperature estimates of Ichthyosauria, Plesiosauria, and Metriorhynchidae that are 3°C to 6°C lower than estimated previously (Bernard et al. 2010; Séon et al. 2020; Supplementary Table 2, Supplementary Fig. 5).

According to our new estimates, Ichthyosauria maintained their body temperatures at a constant value well above environmental values (Fig. 8A) and can be considered as homeothermic endotherms, consistent with previous isotope-based studies (Bernard et al. 2010; Séon et al. 2022). Nevertheless, the body temperature values estimated (45 ± 2°C) for the ichthyosaurs of the Slottsmøya Member (*Palvennia hoybergeti* and *Keilhauia* sp.) are higher than those of present-day homeothermic endothermic marine vertebrates, based on a $\delta^{18}O_{sw}$ value of −1.5‰ from the equation of Alberti et al. (2020). However, this equation is calibrated between 0° and 40°N, and it is probable that this $\delta^{18}O_{sw}$ value of −1.5‰ is overestimated, given that ocean basins such as the Arctic Ocean at the time were landlocked and were therefore likely to be subject to freshwater input from precipitation runoff. Estimates from numerical modeling for the middle Cretaceous indicate $\delta^{18}O_{sw}$ values of

https://doi.org/10.1017/pab.2025.2 Published online by Cambridge University Press

−5 ± 2‰ for this region (Zhou et al. 2008). Based on this modeled $\delta^{18}O_{sw}$ value, the estimated body temperature of ichthyosaurs from the Slottsmøya Member would have been 31 ± 4°C, confirming the homeothermic and endothermic nature of Ichthyosauria. In contrast to previous studies, however, our results indicate that Plesiosauria, as well as Metriorhynchidae, had body temperatures higher than but covarying with environmental temperatures, and hence should be considered poikilothermic endotherms. We note that the estimated Metriorhynchidae body temperatures are closer to those of their environmental values than in Plesiosauria (Fig. 8B,C). These thermoregulatory strategies are largely consistent with other indices linked to paleobiogeography, morphology, locomotion, and estimated metabolic rates.

Indeed, Ichthyosauria would have been able to live in high-latitude environments (Delsett et al. 2016; Rogov et al. 2019) where ocean paleotemperatures were too low for ectothermic turtles and crocodylomorphs to survive, as evidenced by their absence in high-latitude deposits from the same stratigraphic levels (Rich et al. 2002; Bardet et al. 2014). This would have been greatly facilitated by their high metabolic rates (de Buffrénil and Mazin 1990; Nakajima et al. 2014; Anderson et al. 2019) and their fusiform morphology, which is very effective in limiting heat loss to the environment (Innes et al. 1990; Gearty et al. 2018), coupled with a subcutaneous layer of adipose tissue reducing thermal conductivity (Lindgren et al. 2018; Delsett et al. 2022). Nevertheless, this could only be the case for the most recent ichthyosaurs in the evolution of the lineage, such as parvipelvian and thunniform ichthyosaurs of the Ophthalmosauridae family. Indeed, primitive Ichthyosauria had more anguiliform morphologies and, as far as we know, no adipose tissue has been found in these specimens (Motani 2005; Moon and Stubbs 2020).

For Plesiosauria, the characterization of their thermoregulatory strategy is more ambiguous, and our results differ interestingly from those for ichthyosaurs and to some extent contrast with previous studies (Bernard et al. 2010; Séon et al. 2020; Leuzinger et al. 2023). High metabolic rates close to those of modern endotherms are supported by the plesiosaurs' paleobiogeographic distribution (Bardet et al. 2014; Delsett et al. 2016; Zverkov et al. 2021), osteo-histological evidence (Wiffen et al. 1995; Kear 2006a; Delsett and Hurum 2012; Fleischle et al. 2018; O'Keefe et al. 2019; Sander and Wintrich 2021), and the identification and quantification of compounds resulting from the degradation of lipids and carbohydrates by infrared spectroscopy (Wiemann et al. 2022). So far, no evidence for a subcutaneous layer of adipose tissue has been reported in Plesiosauria, but this might be a sampling artifact, as specimens exhibiting soft-tissue preservation are exceptionally rare (Vincent et al. 2017). On the other hand, our new data from teeth show that their body temperatures covaried to some extend with environmental temperatures. One possible explanation that may reconcile these apparently contradictory observations is that Plesiosauria produced heat through their locomotor muscles. This heat production strategy is indeed used by sea turtles with the same type of locomotion and enables them to have core body temperatures higher than the rest of the body (Standora et al. 1982; Sato et al. 1994). The heat generated by muscle contraction may then partly be conserved by the inertia of their body mass (gigantothermy), as in the case of leatherback turtles (Paladino et al. 1990; Sato 2014), whose bone histology studies show evidence of elevated growth rate and high metabolic rate (Nakajima et al. 2014; Wilson 2023). The existence of a comparable heat production system in Plesiosauria may thus partly explain the recorded difference between their body temperatures and their environments as well as their inability to maintain their body temperature at a constant level in the thermally least favorable environments (high latitudes).

Metriorhynchidae differed from the previous two in terms of their geographic distribution, which was restricted to tropical zones (Bardet et al. 2014), and show osteo-histological features (Hua and de Buffrénil 1996; de Buffrénil et al. 2021) indicative of a poikilothermic ectothermic thermoregulatory strategy. While Metriorhynchidae were initially considered to be active hunters (Massare 1987; Young and de Andrade 2009; de Andrade et al. 2010; Young et al. 2012), it was later postulated that some species could also have been scavengers and opportunists (Hua et al. 2024), a strategy that does not require the production of long and intense efforts, in agreement with the estimates of their movement speed (Massare 1988; Massare et al. 1994; Gutarra et al. 2023). Although their body temperatures have been considered as slightly higher than those of their environments (Séon et al. 2020), our revised estimates point to much lower differences than previously estimated. Interestingly, Gienger et al. (2017) showed that the standard metabolic rate values measured in saltwater crocodiles (*Crocodylus porosus*) are 36% higher than those of other taxa such as American alligator (*Alligator mississippiensis*) or freshwater crocodile (*Crocodylus johnstoni*). However, this difference in metabolic rate is not visible in the osteo-histological sections taken from these species (de Buffrénil et al. 2021). Metriorhynchidae may therefore have had a higher metabolic rate, but this difference would not be recorded in bone tissue. We therefore speculate that the production of metabolic heat could have been linked to vital organs such as intestines or liver as well as the locomotor muscles, which, as in tuna, would have been internalized and close to the spinal column and would have limited heat loss to the surrounding aquatic environment (Graham and Dickson 2004).

Conclusion

The reassessment of oxygen isotope–based body temperature estimates of Ichthyosauria, Plesiosauria, and Metriorhynchidae have led to a reconsideration of their thermoregulatory strategies. The intraskeletal $\delta^{18}O_p$ variability in four specimens of Ichthyosauria, three specimens of Plesiosauria, and one specimen of *Metriorhynchus* aff. *superciliosus* did not allow us to characterize and locate regional heterothermies. This may be due to the impact of diagenetic processes on the original oxygen isotope composition of bone bioapatite. The newly measured $\delta^{18}O_p$ from the teeth of Ichthyosauria specimens from high paleolatitudes confirms that these organisms had body temperatures higher than those of their living environments and were probably homeothermic endotherms with body temperature ranging between 31°C and 37°C. In contrast to Ichthyosauria, it appears that the body temperatures of Plesiosauria and Metriorhynchidae were influenced by changes in environmental temperatures. Therefore, they were most likely poikilothermic endotherms, such as some extant sea turtles and tunas. Nevertheless, the thermoregulatory strategy of Metriorhynchidae remains difficult to characterize, because their body temperature estimates are very close to those of their environments, and they could be defined as either poikilothermic endotherms or poikilothermic ectotherms. Further investigations are needed to clearly define their thermoregulatory strategy. Finally, the independency of Ichthyosauria body temperatures relative to environmental temperatures, confirmed by our study, places these organisms as promising

https://doi.org/10.1017/pab.2025.2 Published online by Cambridge University Press

tracers of spatiotemporal changes in $\delta^{18}O_{sw}$ values that could allow for improved Mesozoic paleoclimate reconstructions.

Acknowledgments. Stable isotope measurements were performed at the Plateforme d'Ecologie Isotopique du Laboratoire d'Ecologie des Hydrosystèmes Naturels et Anthropisés (LEHNA, UMR5023, Université Claude Bernard Lyon 1, Lyon, France) and Raman spectroscopy analyses at the Plateforme de Spectroscopie Raman du Laboratoire de Géologie de Lyon (LGL-TPE, UMR5276, Université Claude Bernard Lyon 1). The authors warmly thank the heads and the people responsible for the collection of the Natural History Museum of Oslo, Norway, M. Fouché and S. Rajaofera from the Muséum d'Histoire Naturelle d'Auxerre, France, N. Morel from the Muséum d'Histoire Naturelle Le Mans, and Laurent Picot from the Paléospace museum for allowing us to sample specimens in their respective collections. This study was funded by the ANR-OXYMORE (grant no. ANR-18-CE31-0020) and the project 335111 of the Norwegian Research Council. The authors would like to thank the two reviewers for their helpful comments, which helped to improve the article.

Competing Interests. The authors declare no competing interests.

Data Availability Statement. The detailed datasets produced and used for analysis are included as Supplementary Information and Figures on Zenodo (https://zenodo.org/records/14172945), while Supplementary Tables are available on Dryad (https://doi.org/10.5061/dryad.8gtht76zf).

Literature Cited

Alberti, M., F. T. Fürsich, A. A. Abdelhady, and N. Andersen. 2017. Middle to Late Jurassic equatorial seawater temperatures and latitudinal temperature gradients based on stable isotopes of brachiopods and oysters from Gebel Maghara, Egypt. *Palaeogeography, Palaeoclimatology, Palaeoecology* **468**: 301–313.

Alberti, M., Y. Leshno, F. T. Fürsich, Y. Edelman-Furstenberg, N. Andersen, and D. Garbe-Schönberg. 2020. Stress in the tropics? Impact of a latitudinal seawater $\delta^{18}O$ gradient on Middle Jurassic temperature reconstructions at low latitudes. *Geology* **48**:1210–1215.

Amiot, R., C. Lécuyer, G. Escarguel, J.-P. Billon-Bruyat, E. Buffetaut, C. Langlois, S. Martin, F. Martineau, and J.-M. Mazin. 2007. Oxygen isotope fractionation between crocodilian phosphate and water. *Palaeogeography, Palaeoclimatology, Palaeoecology* **243**:412–420.

Anderson, K. L., P. S. Druckenmiller, G. M. Erickson, and E. E. Maxwell. 2019. Skeletal microstructure of *Stenopterygius quadriscissus* (Reptilia, Ichthyosauria) from the Posidonienschiefer (Posidonia Shale, Lower Jurassic) of Germany. *Palaeontology* **62**:433–449.

Anderson, T. F., B. N. Popp, A. C. Williams, L.-Z. Ho, and J. D. Hudson. 1994. The stable isotopic records of fossils from the Peterborough Member, Oxford Clay Formation (Jurassic), UK: palaeoenvironmental implications. *Journal of the Geological Society* **151**:125–138.

Bardet, N. 1994. Extinction events among Mesozoic marine reptiles. *Historical Biology* **7**:313–324.

Bardet, N., J. Falconnet, V. Fischer, A. Houssaye, S. Jouve, X. P. Suberbiola, A. Pérez-García, J.-C. Rage, and P. Vincent. 2014. Mesozoic marine reptile palaeobiogeography in response to drifting plates. *Gondwana Research* **26**: 869–887.

Barrick, R. E., and W. J. Showers. 1994. Thermophysiology of *Tyrannosaurus rex*: evidence from oxygen isotopes. *Science* **265**:222–224.

Barrick, R. E., A. G. Fischer, Y. Kolodny, B. Luz, D. Bohaska. 1992. Cetacean bone oxygen isotopes as proxies for Miocene ocean composition and glaciation. *Palaios* **7**:521–531.

Barrick, R. E., A. G. Fischer, and W. J. Showers. 1999. Oxygen isotopes from turtle bone: applications for terrestrial paleoclimates? *Palaios*:186–191.

Barthel, H. J., D. Fougerouse, T. Geisler, and J. Rust. 2020. Fluoridation of a lizard bone embedded in Dominican amber suggests open-system behavior. *PLoS ONE* **15**:e0228843.

Bernal, D., J. K. Carlson, K. J. Goldman, and C. G. Lowe. 2012. Energetics, metabolism, and endothermy in sharks and rays. *Biology of Sharks and Their Relatives* **211**:237.

Bernard, A., C. Lécuyer, P. Vincent, R. Amiot, N. Bardet, E. Buffetaut, G. Cuny, et al. 2010. Regulation of body temperature by some Mesozoic marine reptiles. *Science* **328**:1379–1382.

Blainville, H.-M.D. 1835. Description de quelques espèces de reptiles de la Californie, précédée de l'analyse d'un système général d'erpétologie et d'amphibiologie. *Nouvelles Annales du Muséum d'Histoire Naturelle Paris* **4**:233–296.

Blake, R. E., J. R. O'Neil, and G. A. Garcia. 1997. Oxygen isotope systematics of biologically mediated reactions of phosphate: I. Microbial degradation of organophosphorus compounds. *Geochimica et Cosmochimica Acta* **61**: 4411–4422.

Blank, J. M., J. M. Morrissette, C. J. Farwell, M. Price, R. J. Schallert, and B. A. Block. 2007. Temperature effects on metabolic rate of juvenile Pacific bluefin tuna *Thunnus orientalis*. *Journal of Experimental Biology* **210**: 4254–4261.

Block, B. 1987. Billfish brain and eye heater: a new look at non-shivering heat production. *Physiology* **2**:208–213.

Block, B. A. 1986. Structure of the brain and eye heater tissue in marlins, sailfish, and spearfishes. *Journal of Morphology* **190**:169–189.

Block, B. A., and J. R. Finnerty. 1994. Endothermy in fishes: a phylogenetic analysis of constraints, predispositions, and selection pressures. *Environmental Biology of Fishes* **40**:283–302.

Brice, P., and G. Grigg. 2023. Modeling gigantothermy endorses the whole-body tachymetabolic endothermy of ichthyosaurs, mosasaurs, and plesiosaurs (Sauropsida). P. **312** in H. N. Woodward Ballard and J. O. Farlow, eds. *Ruling reptiles: crocodylian biology and archosaur paleobiology*. Indiana University Press, Bloomington.

Brisson, M. J. 1762. *Regnum animale in classes IX distributum, sive synopsis methodica sistens classium, quadripedum scilicet & cetaceorum, particularum divisionem in ordines, sectiones, genera & species*. Editio Altera Auctior. Theodorum Haak Lugduni Batavorum, Leiden.

Brudevold, F., and R. Soremark. 1967. Chemistry of the mineral phase of enamel. *Structural and Chemical Organization of Teeth* **2**:247–277.

Buchy, M., E. Frey, and S. W. Salisbury. 2006. The internal cranial anatomy of the Plesiosauria (Reptilia, Sauropterygia): evidence for a functional secondary palate. *Lethaia* **39**:289–303.

Campos, L., M. S. Fernández, and Y. Herrera. 2020. A new ichthyosaur from the Late Jurassic of north-west Patagonia (Argentina) and its significance for the evolution of the narial complex of the ophthalmosaurids. *Zoological Journal of the Linnean Society* **188**:180–201.

Carey, F. G. 1982. A brain heater in the swordfish. *Science* **216**:1327–1329.

Chenery, C., G. Müldner, J. Evans, H. Eckardt, and M. Lewis. 2010. Strontium and stable isotope evidence for diet and mobility in Roman Gloucester, UK. *Journal of Archaeological Science* **37**:150–163.

Clarke, A., and H. Pörtner. 2010. Temperature, metabolic power and the evolution of endothermy. *Biological Reviews* **85**:703–727.

Coplen, T. B., W. A. Brand, M. Gehre, M. Gröning, H. A. J. Meijer, B. Toman, and R. M. Verkouteren. 2006. New guidelines for $\delta^{13}C$ measurements. *Analytical Chemistry* **78**:2439–2441.

Cowgill, T., M. T. Young Fls, J. A. Schwab, S. Walsh, L. M. Witmer, Y. Herrera, K. N. Dollman, A. H. Turner, and S. L. Brusatte. 2023. Cephalic salt gland evolution in Mesozoic pelagic crocodylomorphs. *Zoological Journal of the Linnean Society* **197**:812–835.

Crowson, R. A., W. J. Showers, E. K. Wright, and T. C. Hoering. 1991. Preparation of phosphate samples for oxygen isotope analysis. *Analytical Chemistry* **63**:2397–2400.

Dal Sasso, G., I. Angelini, L. Maritan, and G. Artioli. 2018. Raman hyperspectral imaging as an effective and highly informative tool to study the diagenetic alteration of fossil bones. *Talanta* **179**:167–176.

de Andrade, M. B., M. T. Young, J. B. Desojo, and S. L. Brusatte. 2010. The evolution of extreme hypercarnivory in Metriorhynchidae (Mesoeucrocodylia: Thalattosuchia) based on evidence from microscopic denticle morphology. *Journal of Vertebrate Paleontology* **30**:1451–1465.

de Buffrénil, V., and J. Mazin. 1989. Bone histology of *Claudiosaurus germaini* (Reptilia, Claudiosauridae) and the problem of pachyostosis in aquatic tetrapods. *Historical Biology* **2**:311–322.

de Buffrénil, V., and J.-M. Mazin. 1990. Bone histology of the ichthyosaurs: comparative data and functional interpretation. *Paleobiology* **16**:435–447.

de Buffrénil, V., M. Laurin, and S. Jouve. 2021. Archosauromorpha: the Crocodylomorpha. Pp. 486–510 *in* V. de Buffrénil, A. J. de Ricqlès, L. Zylberberg, and K. Padian, eds. *Vertebrate skeletal histology and paleohistology*. CRC Press, Boca Raton, Fla.

Delsett, L. L., and J. H. Hurum. 2012. Gross internal structure and microstructure of plesiosaur limb bones from the Late Jurassic, central Spitsbergen. *Norwegian Journal of Geology/Norsk Geologisk Forening* **92**:285–309.

Delsett, L. L., L. K. Novis, A. J. Roberts, M. J. Koevoets, Ø. Hammer, P. S. Druckenmiller, and J. H. Hurum. 2016. The Slottsmøya marine reptile *Lagerstätte*: depositional environments, taphonomy and diagenesis. *Geological Society of London Special Publication* **434**:165–188.

Delsett, L. L., A. J. Roberts, P. S. Druckenmiller, and J. H. Hurum. 2017. A new ophthalmosaurid (Ichthyosauria) from Svalbard, Norway, and evolution of the ichthyopterygian pelvic girdle. *PLoS ONE* **12**:e0169971.

Delsett, L. L., P. S Druckenmiller, A. J. Roberts, and J. H. Hurum. 2018. A new specimen of *Palvennia hoybergeti*: implications for cranial and pectoral girdle anatomy in ophthalmosaurid ichthyosaurs. *PeerJ* **6**:e5776.

Delsett, L. L., A. J. Roberts, P. S. Druckenmiller, and J. H. Hurum. 2019. Osteology and phylogeny of Late Jurassic ichthyosaurs from the Slottsmoya Member Lagerstätte (Spitsbergen, Svalbard). *Acta Palaeontologica Polonica* **64**:4.

Delsett, L. L., H. Friis, M. Kölbl-Ebert, and J. H. Hurum. 2022. The soft tissue and skeletal anatomy of two Late Jurassic ichthyosaur specimens from the Solnhofen archipelago. *PeerJ* **10**:e13173.

Dera, G., B. Brigaud, F. Monna, R. Laffont, E. Pucéat, J.-F. Deconinck, P. Pellenard, M. M. Joachimski, and C. Durlet. 2011. Climatic ups and downs in a disturbed Jurassic world. *Geology* **39**:215–218.

Dickson, K. A., and J. B. Graham. 2004. Evolution and consequences of endothermy in fishes. *Physiological and Biochemical Zoology* **77**:998–1018.

Driessens, F. C., and R. K. Verbeeck. 1990. *Biominerals*. CRC Press, Boca Raton, Fla.

Dunham, A. E., B. W. Grant, and K. L. Overall. 1989. Interfaces between biophysical and physiological ecology and the population ecology of terrestrial vertebrate ectotherms. *Physiological Zoology* **62**:335–355.

Erickson, G. M. 1996. Incremental lines of von Ebner in dinosaurs and the assessment of tooth replacement rates using growth line counts. *Proceedings of the National Academy of Sciences USA* **93**:14623–14627.

Favilla, A. B., M. Horning, and D. P. Costa. 2022. Advances in thermal physiology of diving marine mammals: the dual role of peripheral perfusion. *Temperature* **9**:46–66.

Fernández, M., and Z. Gasparini. 2000. Salt glands in a Tithonian metriorhynchid crocodyliform and their physiological significance. *Lethaia* **33**: 269–276.

Fernández, M., and Z. Gasparini. 2008. Salt glands in the Jurassic metriorhynchid *Geosaurus*: implications for the evolution of osmoregulation in Mesozoic marine crocodyliforms. *Naturwissenschaften* **95**:79–84.

Finger, J. W., Jr., P. C. Thomson, and S. R. Isberg. 2019. A pilot study to understand tooth replacement in near-harvest farmed saltwater crocodiles (*Crocodylus porosus*): implications for blemish induction. *Aquaculture* **504**: 102–106.

Fitzinger, L. 1843. *Systema Reptilium, Fasciculus Primus, Ambyglossae*. Braumüller et Seidel, Vienna.

Fleischle, C. V., T. Wintrich, and P. M. Sander. 2018. Quantitative histological models suggest endothermy in plesiosaurs. *PeerJ* **6**:e4955.

Folkow, L. P., and A. S. Blix. 1987. Nasal heat and water exchange in gray seals. *American Journal of Physiology—Regulatory, Integrative and Comparative Physiology* **253**:R883–R889.

Fourel, F., F. Martineau, C. Lécuyer, H. Kupka, L. Lange, C. Ojeimi, and M. Seed. 2011. $^{18}O/^{16}O$ ratio measurements of inorganic and organic materials by elemental analysis–pyrolysis–isotope ratio mass spectrometry continuous-flow techniques. *Rapid Communications in Mass Spectrometry* **25**:2691–2696.

Fourel, F., F. Martineau, E. Emoke Tóth, A. Görög, G. Escarguel, and C. Lécuyer. 2015. Carbon and oxygen isotope variability among foraminifera and ostracod carbonated shells. *Annales Universitatis Mariae Curie-Skłodowska, sectio AAA–Physica* 70.

Fricke, H. C., W. C. Clyde, J. R. O'Neil, and P. D. Gingerich. 1998. Evidence for rapid climate change in North America during the latest Paleocene thermal maximum: oxygen isotope compositions of biogenic phosphate from the Bighorn Basin (Wyoming). *Earth and Planetary Science Letters* **160**: 193–208.

Friedman, I., J. O'Neil, and G. Cebula. 1982. Two new carbonate stable-isotope standards. *Geostandards Newsletter* **6**:11–12.

Fritsches, K. A., R. W. Brill, and E. J. Warrant. 2005. Warm eyes provide superior vision in swordfishes. *Current Biology* **15**:55–58.

Furukawa, S., W. Chiang, S. Watanabe, H. Hung, H. Lin, H. Yeh, S. Wang, K. Tone, and R. Kawabe. 2015. The first record of peritoneal cavity temperature recording in free-swimming dolphinfish *Coryphaena hippurus* by using archival tags, on the east coast of Taiwan. *Journal of Aquaculture and Marine Biology* **2**:00032.

Gandola, R., E. Buffetaut, N. Monaghan, and G. Dyke. 2006. Salt glands in the fossil crocodile *Metriorhynchus*. *Journal of Vertebrate Paleontology* **26**: 1009–1010.

Gearty, W., C. R. McClain, and J. L. Payne. 2018. Energetic tradeoffs control the size distribution of aquatic mammals. *Proceedings of the National Academy of Sciences USA* **115**:4194–4199.

Gehler, A., T. Tütken, and A. Pack. 2011. Triple oxygen isotope analysis of bioapatite as tracer for diagenetic alteration of bones and teeth. *Palaeogeography, Palaeoclimatology, Palaeoecology* **310**:84–91.

Gienger, C. M., M. L. Brien, C. R. Tracy, S. C. Manolis, G. J. Webb, R. S. Seymour, and K. A. Christian. 2017. Ontogenetic comparisons of standard metabolism in three species of crocodilians. *PLoS ONE* **12**:e0171082.

Graham, J. B., and K. A. Dickson. 2004. Tuna comparative physiology. *Journal of Experimental Biology* **207**:4015–4024.

Green, D. R., G. Olack, and A. S. Colman. 2018. Determinants of blood water $\delta^{18}O$ variation in a population of experimental sheep: implications for paleoclimate reconstruction. *Chemical Geology* **485**:32–43.

Gutarra, S., T. L. Stubbs, B. C. Moon, B. H. Heighton, and M. J. Benton. 2023. The locomotor ecomorphology of Mesozoic marine reptiles. *Palaeontology* **66**:e12645.

Halas, S., and J. Szaran. 2001. Improved thermal decomposition of sulfates to SO_2 and mass spectrometric determination of $\delta^{34}S$ of IAEA SO-5, IAEA SO-6 and NBS-127 sulfate standards. *Rapid Communications in Mass Spectrometry* **15**:1618–1620.

Halas, S., G. Skrzypek, W. Meier-Augenstein, A. Pelc, and H. F. Kemp. 2011. Inter-laboratory calibration of new silver orthophosphate comparison materials for the stable oxygen isotope analysis of phosphates. *Rapid Communications in Mass Spectrometry* **25**:579–584.

Hammer, Ø., H. A. Nakrem, C. T. Little, K. Hryniewicz, M. R. Sandy, J. H. Hurum, P. Druckenmiller, E. M. Knutsen, and M. Høyberget. 2011. Hydrocarbon seeps from close to the Jurassic–Cretaceous boundary, Svalbard. *Palaeogeography, Palaeoclimatology, Palaeoecology* **306**:15–26.

Hampton, I. F. G., G. C. Whittow, J. Szekerczes, and S. Rutherford. 1971. Heat transfer and body temperature in the Atlantic bottlenose dolphin, *Tursiops truncatus*. *International Journal of Biometeorology* **15**:247–253.

Harding, L., A. Jackson, A. Barnett, I. Donohue, L. Halsey, C. Huveneers, C. Meyer, et al. 2021. Endothermy makes fishes faster but does not expand their thermal niche. *Functional Ecology* **35**:1951–1959.

Houssaye, A., T. M. Scheyer, C. Kolb, V. Fischer, and P. M. Sander. 2014. A new look at ichthyosaur long bone microanatomy and histology: implications for their adaptation to an aquatic life. *PLoS ONE* **9**:e95637.

Hua, S., and V. de Buffrénil. 1996. Bone histology as a clue in the interpretation of functional adaptations in the Thalattosuchia (Reptilia, Crocodylia). *Journal of Vertebrate Paleontology* **16**:703–717.

Hua, S., J. Liston, and J. Tabouelle. 2024. The diet of *Metriorhynchus* (Thalattosuchia, Metriorhynchidae): additional discoveries and paleoecological implications. *Fossil Studies* **2**:66–76.

Hut, G. 1987. Consultants' group meeting on stable isotope reference samples for geochemical and hydrological investigations. Report to the Director General. International Atomic Energy Agency, Vienna. http://www.iaea.org/inis/collection/NCLCollectionStore/_Public/18/075/18075746.pdf .

Iacumin, P., H. Bocherens, A. Mariotti, and A. Longinelli. 1996. Oxygen isotope analyses of co-existing carbonate and phosphate in biogenic apatite: a way to monitor diagenetic alteration of bone phosphate? *Earth and Planetary Science Letters* **142**:1–6.

Innes, S., G. A. J. Worthy, D. M. Lavigne, and K. Ronald. 1990. Surface areas of phocid seals. *Canadian Journal of Zoology* **68**:2531–2538.

https://doi.org/10.1017/pab.2025.2 Published online by Cambridge University Press

Irving, L., and J. S. Hart. 1957. The metabolism and insulation of seals as bare-skinned mammals in cold water. *Canadian Journal of Zoology* **35**:497–511.

Kear, B. P. 2006a. Marine reptiles from the Lower Cretaceous of South Australia: elements of a high-latitude cold-water assemblage. *Palaeontology* **49**:837–856.

Kear, B. P. 2006b. Plesiosaur remains from Cretaceous high-latitude non-marine deposits in southeastern Australia. *Journal of Vertebrate Paleontology* **26**:196–199.

Kear, B. P., D. Larsson, J. Lindgren, and M. Kundrat. 2017. Exceptionally prolonged tooth formation in elasmosaurid plesiosaurians. *PLoS ONE* **12**: e0172759.

Keenan, S. W. 2016. From bone to fossil: a review of the diagenesis of bioapatite. *American Mineralogist* **101**:1943–1951.

Kihle, J., J. H. Hurum, and L. Liebe. 2012. Preliminary results on liquid petroleum occurring as fluid inclusions in intracellular mineral precipitates in the vertebrae of *Pliosaurus funkei*. *Norwegian Journal of Geology* **92**: 341–352.

Koch, P. L., N. Tuross, and M. L. Fogel. 1997. The effects of sample treatment and diagenesis on the isotopic integrity of carbonate in biogenic hydroxylapatite. *Journal of Archaeological Science* **24**:417–429.

Kohn, M. J., M. J. Schoeninger, and W. W. Barker. 1999. Altered states: effects of diagenesis on fossil tooth chemistry. *Geochimica et Cosmochimica Acta* **63**: 2737–2747.

Kolb, C., M. R. Sánchez-Villagra, and T. M. Scheyer. 2011. The palaeohistology of the basal ichthyosaur *Mixosaurus* (Ichthyopterygia, Mixosauridae) from the Middle Triassic: palaeobiological implications. *Comptes Rendus Palevol* **10**:403–411.

Kolodny, Y., B. Luz, and O. Navon. 1983. Oxygen isotope variations in phosphate of biogenic apatites, I. Fish bone apatite—rechecking the rules of the game. *Earth and Planetary Science Letters* **64**:398–404.

Kolodny, Y., B. Luz, M. Sander, and W. A. Clemens. 1996. Dinosaur bones: fossils or pseudomorphs? The pitfalls of physiology reconstruction from apatitic fossils. *Palaeogeography, Palaeoclimatology, Palaeoecology* **126**: 161–171.

Kral, A. G., M. Lagos, P. Guagliardo, T. Tütken, and T. Geisler. 2022. Rapid alteration of cortical bone in fresh-and seawater solutions visualized and quantified from the millimeter down to the atomic scale. *Chemical Geology* **609**:121060.

Lebrun, P., and P. Courville. 2013. Le jurassique des falaises des Vaches-Noires. *Fossiles, Revue française de paléontologie, hors série* **4**:16–28.

Lécuyer, C., and J.-P. Flandrois. 2023. Mitigation of the diagenesis risk in biological apatite $\delta^{18}O$ interpretation. *Palaeogeography, Palaeoclimatology, Palaeoecology* **630**:111812.

Lécuyer, C., P. Grandjean, J. R. O'Neil, H. Cappetta, and F. Martineau. 1993. Thermal excursions in the ocean at the Cretaceous–Tertiary boundary (northern Morocco): $\delta^{18}O$ record of phosphatic fish debris. *Palaeogeography, Palaeoclimatology, Palaeoecology* **105**:235–243.

Lécuyer, C., C. Bogey, J.-P. Garcia, P. Grandjean, J.-A. Barrat, M. Floquet, N. Bardet, and X. Pereda-Superbiola. 2003. Stable isotope composition and rare earth element content of vertebrate remains from the Late Cretaceous of northern Spain (Laño): did the environmental record survive? *Palaeogeography, Palaeoclimatology, Palaeoecology* **193**:457–471.

Lécuyer, C., R. Amiot, A. Touzeau, and J. Trotter. 2013. Calibration of the phosphate $\delta^{18}O$ thermometer with carbonate–water oxygen isotope fractionation equations. *Chemical Geology* **347**:217–226.

Lee-Thorp, J., and M. Sponheimer. 2003. Three case studies used to reassess the reliability of fossil bone and enamel isotope signals for paleodietary studies. *Journal of Anthropological Archaeology* **22**:208–216.

LeGeros, R. Z. 1981. Apatites in biological systems. *Progress in Crystal Growth and Characterization* **4**:1–45.

LeGrande, A. N., and G. A. Schmidt. 2006. Global gridded data set of the oxygen isotopic composition in seawater. *Geophysical Research Letters* **33**: 2006GL026011.

Le Mort, J., J. E. Martin, L. Picot, and S. Hua. 2022. First description of the most complete *Metriorhynchus* aff. *superciliosus* (Thalattosuchia) specimen from the Callovian of the Vaches-Noires cliffs (Normandy, France) and limitations in the classification of Metriorhynchidae. *Annales de Paléontologie* **108**:102539.

Letulle, T., G. Suan, M. Daëron, M. Rogov, C. Lécuyer, A. Vinçon-Laugier, B. Reynard, G. Montagnac, O. Lutikov, and J. Schlögl. 2022. Clumped isotope evidence for Early Jurassic extreme polar warmth and high climate sensitivity. *Climate of the Past Discussions* **2022**:1–18.

Letulle, T., D. Gaspard, M. Daëron, F. Arnaud-Godet, A. Vinçon-Laugier, G. Suan, and C. Lécuyer. 2023. Multi-proxy assessment of brachiopod shell calcite as a potential archive of seawater temperature and oxygen isotope composition. *Biogeosciences* **20**:1381–1403.

Leuzinger, L., L. Kocsis, Z. Luz, T. Vennemann, A. Ulyanov, and M. Fernández. 2023. Latest Maastrichtian middle- and high-latitude mosasaurs and fish isotopic composition: carbon source, thermoregulation strategy, and thermal latitudinal gradient. *Paleobiology* **49**:353–373.

Lindgren, J., P. Sjövall, V. Thiel, W. Zheng, S. Ito, K. Wakamatsu, R. Hauff, B. P. Kear, A. Engdahl, and C. Alwmark. 2018. Soft-tissue evidence for homeothermy and crypsis in a Jurassic ichthyosaur. *Nature* **564**:359–365.

Linnæus, C. 1758. *Systema naturæ per regna tria naturæ, secundum classes, ordines, genera, species, cum characteribus, differentiis, synonymis, locis.* Tomus Ed. Decima Reformata 1–41–824 HolmiæSalvius.

Lovegrove, B. G. 2017. A phenology of the evolution of endothermy in birds and mammals. *Biological Reviews* **92**:1213–1240.

Lowenstam, H. A., and S. Weiner. 1989. *On biomineralization*. Oxford University Press, New York.

Markwick, P. J. 1998. Fossil crocodilians as indicators of Late Cretaceous and Cenozoic climates: implications for using palaeontological data in reconstructing palaeoclimate. *Palaeogeography, Palaeoclimatology, Palaeoecology* **137**: 205–271.

Martill, D. 1985. The preservation of marine vertebrates in the Lower Oxford Clay (Jurassic) of central England. *Philosophical Transactions of the Royal Society B* **311**:155–165.

Martin, J. E., R. Amiot, C. Lécuyer, and M. J. Benton. 2014. Sea surface temperature contributes to marine crocodylomorph evolution. *Nature Communications* **5**:4658.

Massare, J. A. 1987. Tooth morphology and prey preference of Mesozoic marine reptiles. *Journal of Vertebrate Paleontology* **7**:121–137.

Massare, J. A. 1988. Swimming capabilities of Mesozoic marine reptiles: implications for method of predation. *Paleobiology* **14**:187–205.

Massare, J. A., L. Maddock, Q. Bone, and J. M. V. Rayner. 1994. Swimming capabilities of Mesozoic marine reptiles: a review. Pp. 133–149 *in* L. Maddock, Q. Bone, and J. M. V. Rayner, eds. *The mechanics and physiology of animal swimming*. Cambridge University Press, Cambridge.

Massare, J. A., W. R. Wahl, and D. R. Lomax. 2021. Narial structures in *Ichthyosaurus* and other Early Jurassic ichthyosaurs as precursors to a completely subdivided naris. *Paludicola* **13**:128–139.

Maxwell, E. E., M. W. Caldwell, and D. O. Lamoureux. 2011a. Tooth histology in the cretaceous ichthyosaur *Platypterygius australis*, and its significance for the conservation and divergence of mineralized tooth tissues in amniotes. *Journal of Morphology* **272**:129–135.

Maxwell, E. E., M. W. Caldwell, D. O. Lamoureux, and L. A. Budney. 2011b. Histology of tooth attachment tissues and plicidentine in *Varanus* (Reptilia: Squamata), and a discussion of the evolution of amniote tooth attachment. *Journal of Morphology* **272**:1170–1181.

Maxwell, E. E., M. W. Caldwell, and D. O. Lamoureux. 2012. Tooth histology, attachment, and replacement in the Ichthyopterygia reviewed in an evolutionary context. *Paläontologische Zeitschrift* **86**:1–14.

Mazin, J.-M., and F. Pavy. 1995. L'Ichtyosaure de Coulangeron (Yonne). Une entreprise délicate. *Bulletin de la Société des Sciences Historiques et Naturelles de l'Yonne* **127**:5–14.

McConnaughey, T. A., J. Burdett, J. F. Whelan, and C. K. Paull. 1997. Carbon isotopes in biological carbonates: respiration and photosynthesis. *Geochimica et Cosmochimica Acta* **61**:611–622.

McCrea, J. M. 1950. On the isotopic chemistry of carbonates and a paleotemperature scale. *Journal of Chemical Physics* **18**:849–857.

McElderry, J.-D. P., P. Zhu, K. H. Mroue, J. Xu, B. Pavan, M. Fang, G. Zhao, E. McNerny, D. H. Kohn, and R. T. Franceschi. 2013. Crystallinity and compositional changes in carbonated apatites: evidence from ^{31}P solid-state NMR, Raman, and AFM analysis. *Journal of Solid State Chemistry* **206**:192–198.

Meister, P., and C. Reyes. 2019. The carbon-isotope record of the sub-seafloor biosphere. *Geosciences* **9**:507.

https://doi.org/10.1017/pab.2025.2 Published online by Cambridge University Press

Montagu, G. 1821. Description of a species of *Delphinus*, which appears to be new. *Memoirs of the Wernerian Natural History Society* **3**:75–82.

Moon, B. C., and T. L. Stubbs. 2020. Early high rates and disparity in the evolution of ichthyosaurs. *Communications Biology* **3**:68.

Morrison, P. 1962. Body temperatures in some Australian mammals. III. Cetacea (Megaptera). *Biological Bulletin* **123**:154–169.

Motani, R. 2005. Evolution of fish-shaped reptiles (Reptilia: Ichthyopterygia) in their physical environments and constraints. *Annual Review of Earth and Planetary Sciences* **33**:395–420.

Nakajima, Y., A. Houssaye, and H. Endo. 2014. Osteohistology of the Early Triassic ichthyopterygian reptile *Utatsusaurus hataii*: implications for early ichthyosaur biology. *Acta Palaeontologica Polonica* **59**:343–352.

Nemliher, J. G., G. N. Baturin, T. E. Kallaste, and I. O. Murdmaa. 2004. Transformation of hydroxyapatite of bone phosphate from the ocean bottom during fossilization. *Lithology and Mineral Resources* **39**:468–479.

O'Gorman, J. P., and Z. Gasparini. 2013. Revision of *Sulcusuchus erraini* (Sauropterygia, Polycotylidae) from the Upper Cretaceous of Patagonia, Argentina. *Alcheringa: An Australasian Journal of Palaeontology* **37**:163–176.

O'Keefe, F. R., P. M. Sander, T. Wintrich, and S. Werning. 2019. Ontogeny of polycotylid long bone microanatomy and histology. *Integrative Organismal Biology* **1**:oby007.

Paladino, F. V., M. P. O'Connor, and J. R. Spotila. 1990. Metabolism of leatherback turtles, gigantothermy, and thermoregulation of dinosaurs. *Nature* **344**:858–860.

Páramo-Fonseca, M. E., C. D. Benavides-Cabra, and I. E. Gutiérrez. 2019. A new specimen of *Stenorhynchosaurus munozi* Páramo-Fonseca et al., 2016 (Plesiosauria, Pliosauridae), from the Barremian of Colombia: new morphological features and ontogenetic implications. *Journal of Vertebrate Paleontology* **39**:e1663426.

Passey, B. H., T. F. Robinson, L. K. Ayliffe, T. E. Cerling, M. Sponheimer, M. D. Dearing, B. L. Roeder, and J. R. Ehleringer. 2005. Carbon isotope fractionation between diet, breath CO_2, and bioapatite in different mammals. *Journal of Archaeological Science* **32**:1459–1470.

Passey, B. H., T. E. Cerling, and N. E. Levin. 2007. Temperature dependence of oxygen isotope acid fractionation for modern and fossil tooth enamels. *Rapid Communications in Mass Spectrometry* **21**:2853–2859.

Pasteris, J. D., B. Wopenka, and E. Valsami-Jones. 2008. Bone and tooth mineralization: why apatite? *Elements* **4**:97–104.

Pellegrini, M., J. A. Lee-Thorp, and R. E. Donahue. 2011. Exploring the variation of the $\delta^{18}O_p$ and $\delta^{18}O_c$ relationship in enamel increments. *Palaeogeography, Palaeoclimatology, Palaeoecology* **310**:71–83.

Pucéat, E., B. Reynard, and C. Lécuyer. 2004. Can crystallinity be used to determine the degree of chemical alteration of biogenic apatites? *Chemical Geology* **205**:83–97.

Rash, R., and H. B. Lillywhite. 2019. Drinking behaviors and water balance in marine vertebrates. *Marine Biology* **166**:122.

Reisdorf, A. G., R. Bux, D. Wyler, M. Benecke, C. Klug, M. W. Maisch, P. Fornaro, and A. Wetzel. 2012. Float, explode or sink: postmortem fate of lung-breathing marine vertebrates. *Palaeobiodiversity and Palaeoenvironments* **92**:67–81.

Rich, T. H., P. Vickers-Rich, and R. A. Gangloff. 2002. Polar dinosaurs. *Science* **295**:979–980.

Roberts, A. J., P. S. Druckenmiller, L. L. Delsett, and J. H. Hurum. 2017. Osteology and relationships of *Colymbosaurus* Seeley, 1874, based on new material of *C. svalbardensis* from the Slottsmøya Member, Agardhfjellet Formation of central Spitsbergen. *Journal of Vertebrate Paleontology* **37**: e1278381.

Rogov, M. A., N. G. Zverkov, V. A. Zakharov, and M. S. Arkhangelsky. 2019. Marine reptiles and climates of the Jurassic and Cretaceous of Siberia. *Stratigraphy and Geological Correlation* **27**:398–423.

Sander, P. M., and T. Wintrich. 2021. Sauropterygia: histology of Plesiosauria. Pp. 444–457 *in* V. de Buffrénil, A. J. de Ricqlès, L. Zylberberg, and K. Padian, eds. *Vertebrate skeletal histology and paleohistology*. CRC Press, Boca Raton, Fla

Santos, G. M., J. Ferguson, K. Acaylar, K. R. Johnson, S. Griffin, and E. Druffel. 2011. $\Delta^{14}C$ and $\delta^{13}C$ of seawater DIC as tracers of coastal upwelling: a 5-year time series from Southern California. *Radiocarbon* **53**:669–677.

Sato, K. 2014. Body temperature stability achieved by the large body mass of sea turtles. *Journal of Experimental Biology* **217**:3607–3614.

Sato, K., W. Sakamoto, Y. Matsuzawa, H. Tanaka, and Y. Naito. 1994. Correlation between stomach temperatures and ambient water temperatures in free-ranging loggerhead turtles, *Caretta caretta*. *Marine Biology* **118**: 343–351.

Séon, N. 2023. Détermination des stratégies thermorégulatrices des vertébrés marins actuels et fossiles par les isotopes de l'oxygène: implications paléoenvironnementales. Ph.D. thesis. Muséum national d'Histoire naturelle-MNHN, Paris.

Séon, N., R. Amiot, J. E. Martin, M. T. Young, H. Middleton, F. Fourel, L. Picot, X. Valentin, and C. Lécuyer. 2020. Thermophysiologies of Jurassic marine crocodylomorphs inferred from the oxygen isotope composition of their tooth apatite. *Philosophical Transactions of the Royal Society B* **375**: 20190139.

Séon, N., R. Amiot, G. Suan, C. Lécuyer, F. Fourel, F. Demaret, A. Vinçon-Laugier, S. Charbonnier, and P. Vincent. 2022. Intra-skeletal variability in phosphate oxygen isotope composition reveals regional heterothermies in marine vertebrates. *Biogeosciences* **19**:2671–2681.

Séon, N., I. Brasseur, C. Scala, T. Tacail, S. Catteau, F. Fourel, P. Vincent, et al. 2023. Determination of water balance maintenance in *Orcinus orca* and *Tursiops truncatus* using oxygen isotopes. *Journal of Experimental Biology* **226**:jeb245648.

Séon, N., R. Amiot, G. Suan, C. Lécuyer, F. Fourel, A. Vinçon-Laugier, S. Charbonnier, and P. Vincent. 2024. Regional heterothermies recorded in the oxygen isotope composition of harbour seal skeletal elements. *Journal of Thermal Biology* **120**:103825.

Sillen, A., and R. LeGeros. 1991. Solubility profiles of synthetic apatites and of modern and fossil bones. *Journal of Archaeological Science* **18**:385–397.

Sisma-Ventura, G., T. Tütken, S. T. M. Peters, O. M. Bialik, I. Zohar, and A. Pack. 2019. Past aquatic environments in the Levant inferred from stable isotope compositions of carbonate and phosphate in fish teeth. *PLoS ONE* **14**: e0220390.

Standora, E. A., J. R. Spotila, and R. E. Foley. 1982. Regional endothermy in the sea turtle, *Chelonia mydas*. *Journal of Thermal Biology* **7**:159–165.

Stubbs, T. L., and M. J. Benton. 2016. Ecomorphological diversifications of Mesozoic marine reptiles: the roles of ecological opportunity and extinction. *Paleobiology* **42**:547–573.

Takashima, R., H. Nishi, B. T. Huber, and R. M. Leckie. 2006. Greenhouse world and the Mesozoic ocean. *Oceanography* **19**(4):82–92.

Thomas, D. B., R. E. Fordyce, R. D. Frew, and K. C. Gordon. 2007. A rapid, non-destructive method of detecting diagenetic alteration in fossil bone using Raman spectroscopy. *Journal of Raman Spectroscopy* **38**:1533–1537.

Thomas, D. B., C. M. McGoverin, R. E. Fordyce, R. D. Frew, and K. C. Gordon. 2011. Raman spectroscopy of fossil bioapatite—a proxy for diagenetic alteration of the oxygen isotope composition. *Palaeogeography, Palaeoclimatology, Palaeoecology* **310**:62–70.

Trueman, C., C. Chenery, D. A. Eberth, and B. Spiro. 2003. Diagenetic effects on the oxygen isotope composition of bones of dinosaurs and other vertebrates recovered from terrestrial and marine sediments. *Journal of the Geological Society* **160**:895–901.

Turner-Walker, G., A. G. Galiacho, N. Armentano, and C.-Q. Hsu. 2023. Bacterial bioerosion of bones is a post-skeletonisation phenomenon and appears contingent on soil burial. *Quaternary International* **660**:75–83.

Tütken, T., T. W. Vennemann, and H.-U. Pfretzschner. 2008. Early diagenesis of bone and tooth apatite in fluvial and marine settings: constraints from combined oxygen isotope, nitrogen and REE analysis. *Palaeogeography, Palaeoclimatology, Palaeoecology* **266**:254–268.

van Hinsbergen, D. J., L. V. De Groot, S. J. van Schaik, W. Spakman, P. K. Bijl, A. Sluijs, C. G. Langereis, and H. Brinkhuis. 2015. A paleolatitude calculator for paleoclimate studies. *PLoS ONE* **10**:e0126946.

Vavrek, M. J., B. C. Wilhelm, E. E. Maxwell, and H. C. Larsson. 2014. Arctic plesiosaurs from the lower cretaceous of Melville Island, Nunavut, Canada. *Cretaceous Research* **50**:273–281.

Vennemann, T. W., E. Hegner, G. Cliff, and G. W. Benz. 2001. Isotopic composition of recent shark teeth as a proxy for environmental conditions. *Geochimica et Cosmochimica Acta* **65**:1583–1599.

https://doi.org/10.1017/pab.2025.2 Published online by Cambridge University Press

Vincent, P., N. Bardet, and N. Morel. 2007. An elasmosaurid plesiosaur from the Aalenian (Middle Jurassic) of western France. *Neues Jahrbuch für Geologie und Paläontologie, Abhandlungen* **243**:363–370.

Vincent, P., R. Allemand, P. D. Taylor, G. Suan, and E. E. Maxwell. 2017. New insights on the systematics, palaeoecology and palaeobiology of a plesiosaurian with soft tissue preservation from the Toarcian of Holzmaden, Germany. *Science of Nature* **104**:51.

Wahl, W. R. 2012. Salt gland structures identified in a Late Jurassic ichthyosaur *Ophthalmosaurus natans*. *Paludicola* **8**:252–262.

Watanabe, Y. Y., K. J. Goldman, J. E. Caselle, D. D. Chapman, and Y. P. Papastamatiou. 2015. Comparative analyses of animal-tracking data reveal ecological significance of endothermy in fishes. *Proceedings of the National Academy of Sciences USA* **112**:6104–6109.

Wiemann, J., I. Menéndez, J. M. Crawford, M. Fabbri, J. A. Gauthier, P. M. Hull, M. A. Norell, and D. E. Briggs. 2022. Fossil biomolecules reveal an avian metabolism in the ancestral dinosaur. *Nature* **606**:522–526.

Wierzbowski, H., M. A. Rogov, B. A. Matyja, D. Kiselev, and A. Ippolitov. 2013. Middle–Upper Jurassic (Upper Callovian–Lower Kimmeridgian) stable isotope and elemental records of the Russian Platform: indices of oceanographic and climatic changes. *Global and Planetary Change* **107**:196–212.

Wiffen, J., V. De Buffrénil, A. De Ricqlès, and J.-M. Mazin. 1995. Ontogenetic evolution of bone structure in Late Cretaceous Plesiosauria from New Zealand. *Geobios* **28**:625–640.

Wilson, L. E. 2023. Rapid growth in Late Cretaceous sea turtles reveals life history strategies similar to extant leatherbacks. *PeerJ* **11**:e14864.

Wingender, B., M. Azuma, C. Krywka, P. Zaslansky, J. Boyle, and A. Deymier. 2021. Carbonate substitution significantly affects the structure and mechanics of carbonated apatites. *Acta Biomaterialia* **122**:377–386.

Yeates, L. C., and D. S. Houser. 2008. Thermal tolerance in bottlenose dolphins (*Tursiops truncatus*). *Journal of Experimental Biology* **211**:3249–3257.

Young, M. T., and M. B. de Andrade. 2009. What is *Geosaurus*? Redescription of *Geosaurus giganteus* (Thalattosuchia: Metriorhynchidae) from the Upper Jurassic of Bayern, Germany. *Zoological Journal of the Linnean Society* **157**:551–585.

Young, M. T., S. L. Brusatte, M. B. De Andrade, J. B. Desojo, B. L. Beatty, L. Steel, M. S. Fernández, M. Sakamoto, J. I. Ruiz-Omeñaca, and R. R. Schoch. 2012. The cranial osteology and feeding ecology of the metriorhynchid crocodylomorph genera *Dakosaurus* and *Plesiosuchus* from the Late Jurassic of Europe. *PLoS ONE* **7**:e44985.

Zazzo, A., C. Lécuyer, and A. Mariotti. 2004a. Experimentally-controlled carbon and oxygen isotope exchange between bioapatites and water under inorganic and microbially-mediated conditions. *Geochimica et Cosmochimica Acta* **68**:1–12.

Zazzo, A., C. Lécuyer, S. M. Sheppard, P. Grandjean, and A. Mariotti. 2004b. Diagenesis and the reconstruction of paleoenvironments: a method to restore original $\delta^{18}O$ values of carbonate and phosphate from fossil tooth enamel. *Geochimica et Cosmochimica Acta* **68**:2245–2258.

Zhou, J., C. J. Poulsen, D. Pollard, and T. S. White. 2008. Simulation of modern and middle Cretaceous marine $\delta^{18}O$ with an ocean-atmosphere general circulation model. *Paleoceanography* **23**:2008PA001596.

Zverkov, N. G., D. V. Grigoriev, and I. G. Danilov. 2021. Early Jurassic palaeopolar marine reptiles of Siberia. *Geological Magazine* **158**:1305–1322.

https://doi.org/10.1017/pab.2025.2 Published online by Cambridge University Press